Real-time River Nile Flow Forecasting by using Mathematical models of Flood Early Warning System in Sudan (FEWS)

Redwan Abdelrhman Mohammed

A DISSERTATION SUBMITTED TO THE UNESCO CHAIR IN WATER RESOURCES OF THE OMDURMAN ISLAMIC UNIVERSITY IN PARTIAL FULFILMENT FOR THE DEGREE OF MASTER OF SCEINCE (M.Sc.) IN WATER RESOURCES DEVELOPMENT AND MANAGEMENT.

UNESCO CHAIR IN WATER RESOURCES

OMDURMAN ISLAMIC UNIVERSITY

September 2008

CERTIFICATION

The undersigned certify that they have read and hereby recommend for examination/acceptance by the UNESCO Chair in Water Resources a thesis/dissertation entitled: *A comparative modelling study in Blue Nile basin*, in fulfilment/partial fulfilment of the requirements for the degree of M.Sc.

_____

Name:Kamal El din E. Bashar

(SUPERVISOR)

Date _____

DECLARATION AND COPYRIGHT

I**, Redwan Abdelrhman Mohammed**, declare that, this thesis is my own original work and that it has not been presented and will not be presented to any other university for a similar or any other degree award.

Signature_____

ACKNOWLEDGEMENT

I would like to thank **Dr. Kamal Bashar** for his advices, guidance and supervision of this thesis..

I wish to record my thanks to **NBI** staff for sponsoring me to get my degree.

I extend my thanks to all, who help me and encourage me to complete this thesis,

FIRST OF ALL I thank MY **GOD** who be beside me.

DEDICATION

To my mother and I ask GOD for more age and

healthy for her

To the memory of my father

To all my family……..,

ABSTRACT

River flood frequency in the Sudan in recent years is increased. In order to protect property and crops with operating small scale water structures flood forecast is necessary.

The objective of the study is to perform rainfall-runoff forecasting with simulation & routing of water flow in river course network using FEWS (Flood Early Warning System) model and then assessment of the FEWS model performance, in comparison to simple routing methods.

Two models are applied for forecasting flow of river Nile at three hydrological stations namely El Diem, Khartoum and Dongola. These models are FEWS model and simple non–storage routing methods (regression between neighbour stations). These models are applied in simulation mode.

Data used for application of the model, is four years (1989-1992) used for calibrating the model, and 2007 used for application.

A comparison based on model statistical values of model efficiency, the higher efficiency is obtained by simple non–storage routing methods as well as statistical significance test. Therefore the methods is recommended to be used for forecasting river along the river Nile course in Sudan.

الخلاصة

وتيرة حدوث فيضانات النيل فى السنين الاخيرة فى السودان باتت فى تكرار متزايد وبالتالى حفاظا للارواح والممتلكات وتشغيل الخزانات لزم وجود النماذج الرياضية للتنبؤ بكمية مياه تصرف الفيضان لأخذ الإحتياطات اللازمة.

الهدف من هذة الدراسة مقارنة نموذجين رياضيين تختصان بالتنبؤ لمعرفة كمية الامطار الساقطة فى الهضبة الاثيوبية وكمية الجريان عند محطة الديم والخرطوم ودنقلا علي النيل.

في هذة الدراسة طبقت نموذجين احدهما نظام الانذار المبكر للفيضان (Flood Early Warning System) والثانى طريقة متابعة الفيضان بالنظام البسيط (simple non-storage routing)

أستخدمت في هذة الدراسة بيانات لخمسة سنوات 1989-1992و2007 لتطبيق تلك الأنمذجة الرياضية. حيث تم استخدام الاربعة سنين الاولى لمعايرة خصائص النموذج واستخدام السنة الاخيرة 2007 للتطبيق.

تمت مقارنة نتائج هذة الأنمذجة الرياضية علي قدرتها لحساب كمية التصرف أقرب إلي التي قيست في المحطات بوسطة القياسين. فوجد ان طريقة متابعة الفيضان بالنظام البسيط (simple non-storage routing) هو الأفضل لحساب كمية التصرف ويمكن من خلال تطبيق هذا الإنموذج للتنبؤ بكمية الجريان في النيل وتقدير كمية مياة الفيضان وعمل الإحتيطات اللازمة.

TABLE OF CONTENTS

Chapter One

Introduction

Chapter Two

Theoretical background to the model

Chapter Three

Material and Method

Chapter Four

Application, Result and Discussion

Chapter Five

Summary, Conclusion and Recommendations

References

Appendix

Appendix 1 Model parameters

List Figure

List of Tables

Chapter One
Introduction

1.0 General

1.1 Background

Flood is an inundation of area and the area remains under water for some time. Inundation causes damage to property and crops disrupt communication and bring harmful effects to human life as disease break out (malaria) as well as to flora and fauna. The river flood is the most common type of flooding, and can be defined as when the actual amount of river flow is larger than the amount that the channel can hold. Then the river will overflow its banks and flood the areas along its side. This may cause by reasons like heavy rain on river catchments or snow melt. In Sudan severe flood frequency happened in 1946, 1988, 1994, 1998 and 2006 in Khartoum area, in 1965 White Nile at Sudd region. An inundation alongside the river has advantages also like support basin irrigation, fish, hydropower generation, groundwater recharge and navigation.

Flood protection systems in Sudan it have different types:

- using Dams to break the peak of the flood wave, regulate the river flow and give the chance to rain water drain to river course however this method of flood protection let the sediment accumulate upstream the dams and economically not easy to remove.

- Embankment of the river bank either earth embankment or concrete embankment are used along the river side narrowing the channel and giving more area protected in the neighborhood but economically not workable when the channel is full the water level rise above the neighbor area and the critical case when a heavy rain happen around the area.

- Using media to alert people to evacuate places of expected inundation. This can be verified by using modern mathematical models and remote sensing technique. It's more economically method and practical.

The Nile Flood Early Warning System Sudan (FEWS) is a set of mathematical models. The importance of early flood warning and improved flood management is increasingly recognized. Damage due to flooding tends to increase with increasing development in river basins, whereas population pressure in flood prone areas is often high. Full protection through large-scale embankments of rivers is often not possible because of prohibitive costs, or even not desirable because of environmental and other reasons. Flood early warning then becomes instrumental in saving lives and property. It may also substantially contribute to improved flood management through more adequate reservoir operation.

1.2 Description of River System and study area
1.2.1 Blue Nile

The Blue Nile and its tributaries all raise on the Ethiopian Plateau at an elevation of 2,000 to 3,000 meters above M.S.L. The little Abay, which enters Lake Tana at 1,829 meters above M.S.L, is generally considered as the source of the Blue Nile. The river passes a deep gorge through the Ethiopian Plateau, which is in some places 1,200 meters below the terrain level on either side. Numerous rock-outcrops occurred in the river bed, the last of which is a few kilometers south of Roseires, some 1,000 km from its source beyond Lake Tana, and known as the Damazin rapids.

The Blue Nile emerges from the Plateau close to the western border of Ethiopia, where it turns north-west and enters the Sudan at an altitude of 490 meters above M.L.S. Just before crossing the frontier, the river enters the clay plain, through which it flows over a distance of about 735 km to Khartoum. At this point the Blue Nile joins the White Nile to form the main system of the Nile River. The average slope of the river between Lake Tana and the Ethiopian frontier is about 1.6m/km. From the frontier to Khartoum the slope is much less, about 15cm/km.

Downstream of the frontier two tributaries of some importance join the Blue Nile in the reach between Sennar and Wad Medani, namely the Dinder and Rahad Rivers. Both rivers originate from the Ethiopian Plateau, about 30 km west of Lake Tana. They are seasonal streams, reduced to pools in the dry season.

The Blue Nile Basin, including the Dinder and Rahad Basins, has a catchments area of 324,530 km^2. The greater part of this catchment is located in Ethiopia.

Two dams have been constructed on the Blue Nile, one at Sennar and one at Roseires, respectively at some 350 and 620 km south east from Khartoum.

The Sennar dam was completed in 1925, for an initial storage capacity of about 0.9 milliard m^3. By now 2007 its live storage has been reduced to about 0.64 milliard m^3, according to a recent bathymetric survey by dams in 2006. The dam has been constructed for irrigation of the Gezirah scheme.

The Roseires reservoir, completed in 1966 with an initial storage capacity of 3 milliard m^3, is operated in conjunction with Sennar with the purpose of satisfying the irrigation requirements upstream and downstream of the dam, and generating the maximum possible power. At later stage the volume of the reservoir was upgraded to about 3.35 milliard m^3. To avoid silt accumulation of the reservoirs as much as possible, filling is delayed to the latest possible time during the falling of flow hydrograph. Now 2007 the life storage of Roseires reservoir has been reduced to about 1.9 milliard m^3.

1.2.2 White Nile

Due to losses in the sudd area, the White Nile pass the area only with 14 milliards m^3, and receive approximately the same amount from the Sobat before joining Blue Nile at Khartoum. The average annual flow of the White Nile System at Jebel Aulia is about 26 milliard m^3 and daily discharge fluctuates between 50 millions in April to 110 million m^3 in November (1:20 ratio low to peak flow). During the flood period the Blue Nile forms natural dam that obstruct the White Nile and consequently flood the area upstream the confluence (Barsi, 1986)

On the White Nile, at about 40 km upstream of Khartoum, the Jebel Aulia dam was constructed in 1937. The initial storage capacity of the reservoir was 3.5 milliard m^3, but since then this has been reduced. Due to the very small slope of the White Nile between Khartoum and Malakal (about 1.4 cm/km), the backwater of the reservoir reaches for more than 400 km upstream of Jebel Aulia.

1.2.3 Atbara River

The river Atbara, which is the last tributary of the Nile, enters the Main Nile at about 320km downstream of Khartoum. It is 880 km long and its catchments area amounts to 112,400 km^2, the greater part of which is situated in Ethiopia. The main tributary of the Atbara is the Setit River, with a catchments area of 69,000 km^2. Over its first 300 km the slope of the Atbara is very steep, i.e. about 5m/km. Below the Setit junction the river runs over a distance of about 500 km at a slope of about 25 cm/km.

The Atbara River is more strongly seasonal in its flow compared to the Blue Nile. The steep slope in its upper reach is responsible for the excessive sediment load of the Atbara River in proportion to its flow volume.

At khashm el Girba, about 440 km upstream of the Atbara mouth, a dam has been constructed. The main objective of the reservoir is to supply the irrigation canals of the New Halfa scheme. The initial storage capacity of the dam in (1964) was 1.3 milliard m^3, which according to a recent bathymetric survey has been reduced to about 0.6 milliard m^3.

1.2.4 Main Nile

At Khartoum the Blue Nile joins the White Nile and the combined waters flow for some 1,850 km to Aswan. The river course consists of a series of placid reaches of mild slope, separated by rocky rapids, called the Cataracts, where the slope is greater and the flow is more turbulent. In the reach down to Dongola 3 cataracts, viz. the 4th Cataract near Merowe, the 5th Cataract between Atbara and Abu Hamed and the Sabaluga or 6th Cataract between Khartoum and Shendi.

The downstream boundary of the flood forecasting model is located at Dongola. The overall average slope between Khartoum and Dongola is of the order of 12 cm/km.

1.2.5 Rainfall

Rainfall in the Ethiopian catchments exceeds by far the rainfall over the Sudanese catchments in the project area. Historic isohyetal maps of the Ethiopian catchments indicate annual values of about 1,000 mm around Lake Tana to 1,500mm towards the South-West.

The annual isohyets for the Sudanese catchments run more or less parallel to the Ethiopian border and show rapid decline towards the North-West. Annual averages rainfall of the isohyets is ranged from 600mm near the Ethiopian border to about 100 mm in the Khartoum region and to less than 10 mm around Dongola. Roughly 90 percent of the rain falls in the period June till September with July and August being the wettest. No rain occurs in the period November-March.

1.3 Selected Stations

In the following subsections, three of the main stations used in FEWS were described. The three selected station to represent the Sudan boarders (entry and exit) with one in central part.

1.3.1 Eddeim station

This station lies on the Ethiopian border. It monitors the inflows to Roseires reservoir and is important for controlling the operation of the Roseires reservoir. It is operated by SMI and was opened in 1962. The channel at Eddiem is a deep rock gorge, which provides a very stable control.

1.3.2 Khartoum station

This site measures the flows of the Blue Nile just above its junction with the White Nile. The record starts in 1900, and is a combination of flows from two sites: high flows are measured at Khartoum itself, while low flows are measured at Soba which is about 25 km upstream.

1.3.3 Dongola station

This station is on the Main Nile downstream of the confluence with the river Atbara, and it is thus the key site which measures the total discharge of the Nile basin as it leaves the Sudan and enters Egypt. The flows are used to monitor the division of the Nile waters between the two countries and the station is operated by staff from both. It was opened in 1962 to replace the previous site further downstream at Wadi Halfa and Kajnarty which was submerged after the construction of the Aswan High dam.

Figure 1.1 shows the Blue Nile catchments while figure 1.2 shows flow gauging stations network in Sudan.
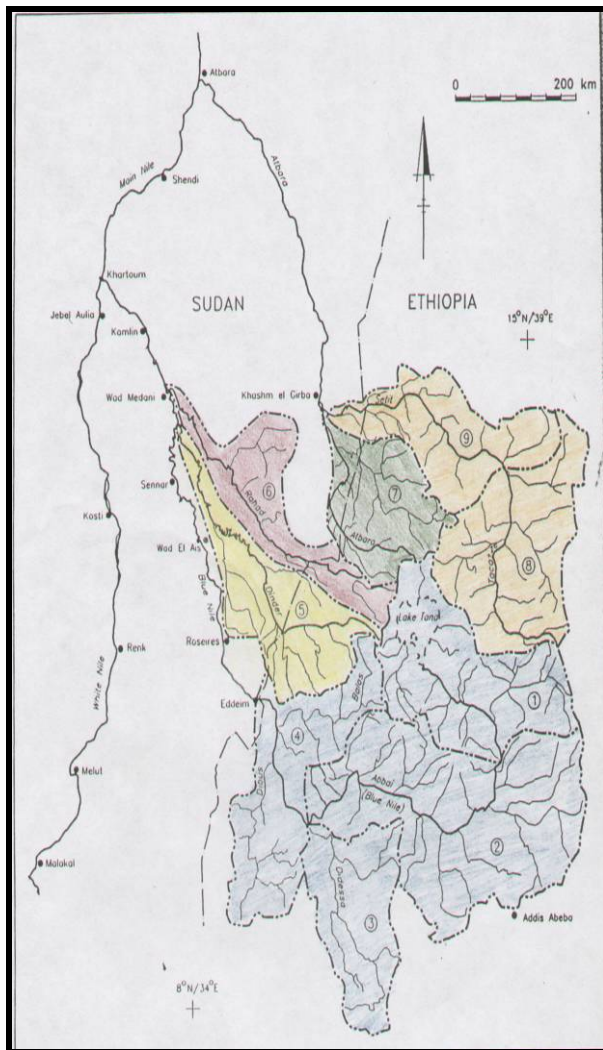
Figure (1.1) shows the upper productive catchments yielding the flow of Blue Nile and Atbara River.
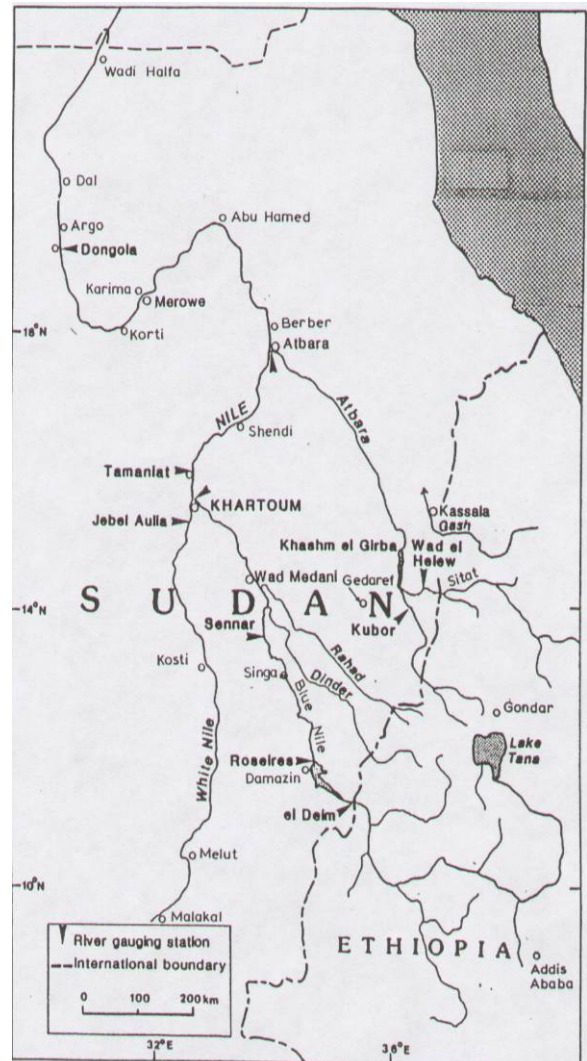
Figure (1.2) shows the gauging station network in the Nile system within Sudan.

1.4 Statement of the problem

In august 1988 a severe flood occurred on the Blue Nile, which caused damage on a massive scale to agriculture, property and infrastructure, in particular in the Khartoum and Northren regions. In the aftermath of this flood DELFT HYDRAULICS was commissioned the preparation and implementation of the Nile FEWS, covering the White Nile, north of Malakal, the entire Blue Nile and Atbara Basins as well as the Main Nile Down to Dongola in the North of the Sudan. The system is implemented at the Ministry of Irrigation and Water Resources in Khartoum, in order to enable more advanced warning for future floods on the Nile, using modern forecasting techniques and improved data collection. The performance of FEWS is not assessed critically since commissioned. This study is an attempt to assess the performance of this system.

1.5 Research Objectives:

The main objectives of this study is to assess the FEWS model performance in the river Nile within the Sudan in providing flow forecasts with a reasonable lead time down stream. This will reduce the flood damages, and enable a good operation of the dams to mange flood beaks. The specific objective includes:

- Perform Rainfall-runoff forecasting using the FEWS models.
- Perform Simulation & Routing of Water flow in river course networks using FEWS model.
- Assess the models performance.

1.6 layout of the thesis

This thesis contains five chapters. The first chapter gives an introduction to the FEWS, overview of river system and description of study area, and the selected stations, statement of the problem and research objectives. The second chapter is dedicated the development in the FEWS modeling, and a short summary about models applied in this study. Chapter three is dedicated for the methodology of operation of the FEWS and analysis of data. Chapter four gives an overviewed for the application, results and discussion. Chapter five is kept for conclusion and recommendations. The end the references are listed.

Chapter Two

Theoretical background to the model

2. 1 Introduction

For further increase in the lead-time for flood forecasting in the Nile basin, use is made of runoff forecasts at time at the upstream boundaries of the river model derived from rainfall in the upper catchments. To this end rainfall-runoff models were developed for the following catchments:

1. Blue Nile upstream of Eddeim,
2. Dinder upstream of Gwasi,
3. Rahad upstream of el Hawata,
4. Atbara upstream of Kubur, and
5. Setit upstream of Wad el Heleiw

The rainfall-runoff process in the catchments of the Blue Nile, the Atara and the Setit were modeled with the SAMO-model, i.e. DELFT HYDRAULICS' upgraded version of the well-known Sacramento model. For forecasting purposes an adapted version of the model is used: SAMO extended with an Extended Kalman Filter to allow a continuous update of the model "state" based on actual measurements. This adapted version is called SAMFIL-model.

For the Rahad and Dinder catchments multiple regression models have been developed to predict the runoff from these catchments.

2.2 SAMO-Model

2.2.1 General

SAMO is an acronym of Sacramento model, which is developed by California Department of Water Resources in 1973. An upgraded of the model called SAMO, for the simulation of the runoff process, the Sacramento model makes a distinction between the land phase and the channel phase. The land phase is represented by explicit moisture accounting lumped parameter model. The catchments area is divided into one or more segments discharge to the main channels, within every segment areal homogeneity with respect to rainfall and basin characteristic is assumed. In the channel phase the

8

propagation and attenuation of flood waves in the channel may be simulated by methods with varying degree of sophistication, ranging from simple summation via unit hydrograph methods to layered routing approaches.

2.2.2 Model concept and components

The concept of the Sacramento model with the major storage and flow component is shown in figure (2.1) and (2.2)
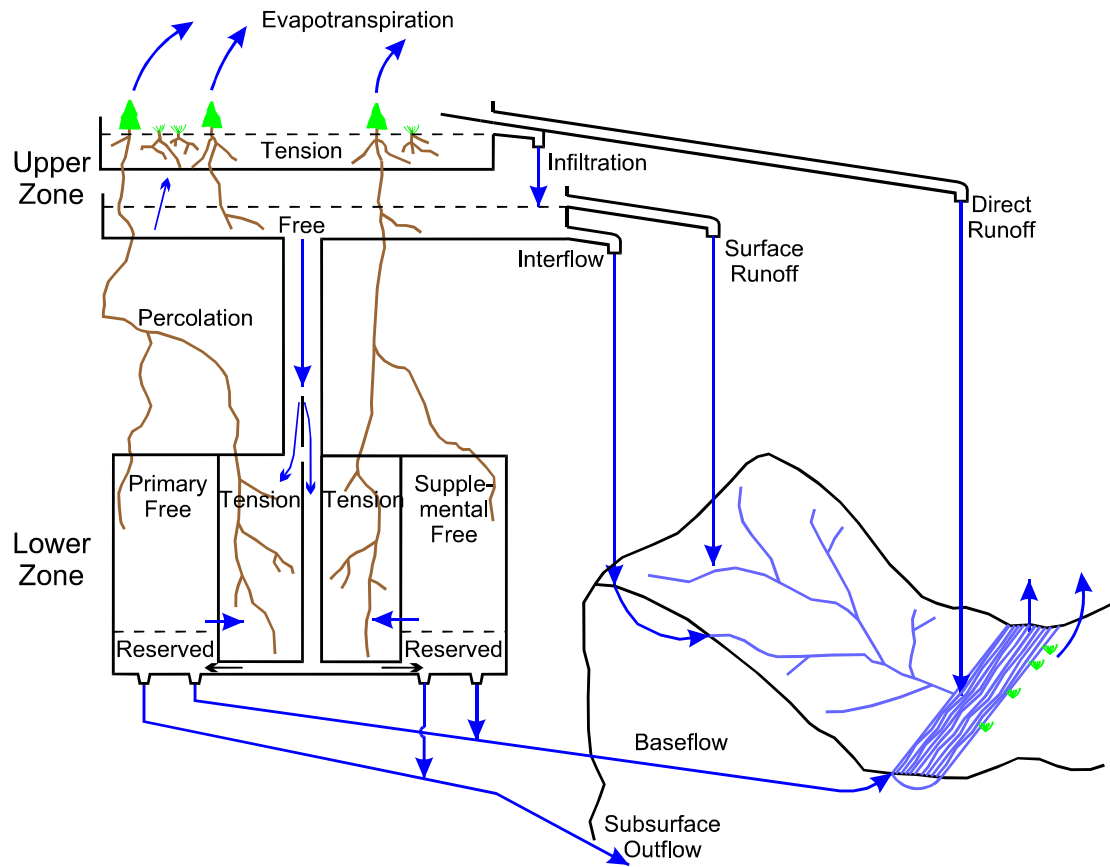
Figure (2.1) concept of the Sacramento model

2.2.3 The land Module

In the land-phase component a distinction is made between the pervious and impervious part of the catchments. From the impervious areas perception immediately discharge to the channel. However, impervious areas, which drain to a pervious part before the water reaches the channel, are not considered as impervious. The drainage system of the pervious part i.e. the main part is divided in:

9
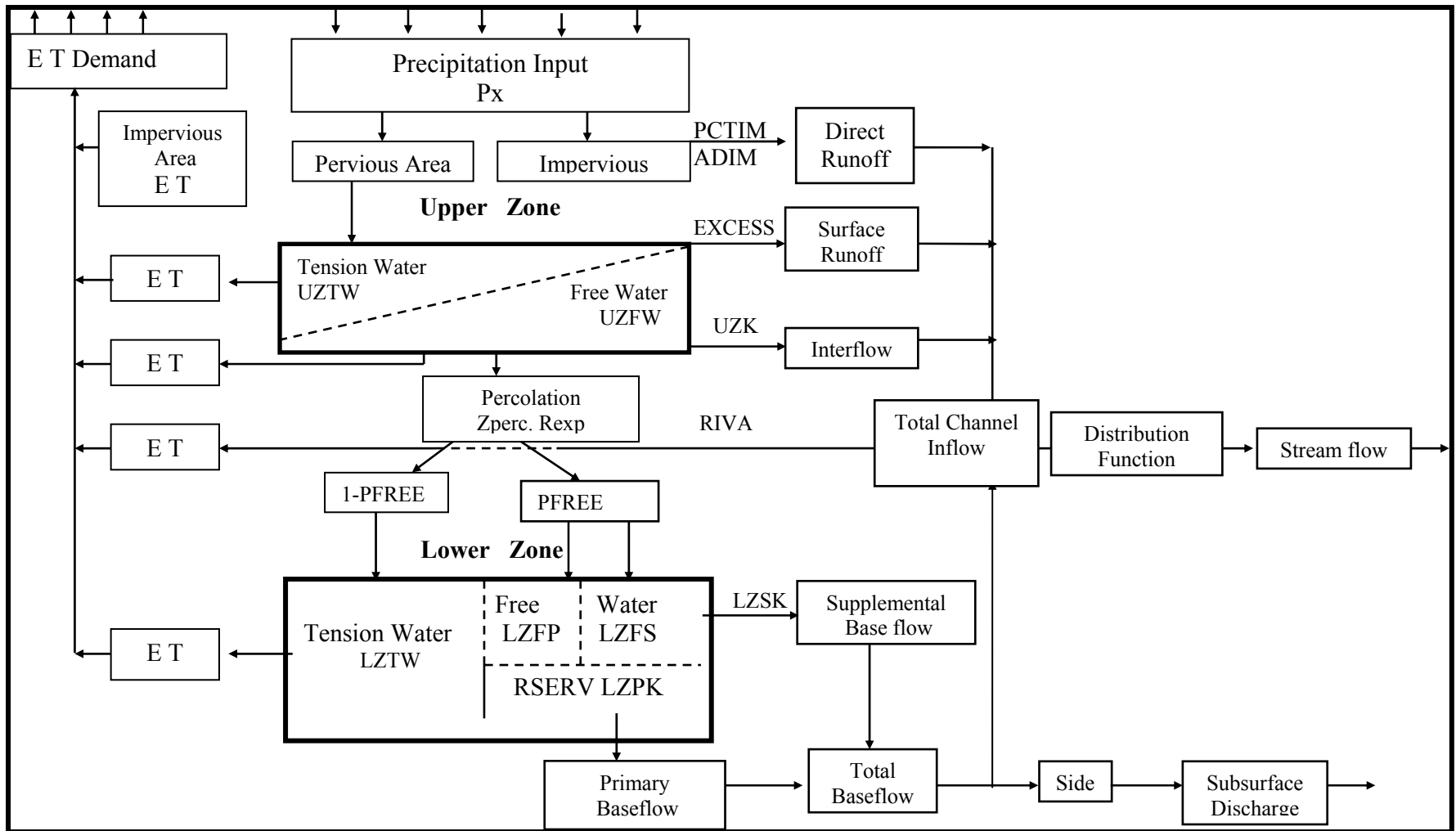
Figure (2.2) Sacramento Model Structure (components)

- An upper zone, representing the catchments surface system;
- A lower zone, representing the catchments groundwater reservoir system.

Both zones have a tension and a free-water storage element. Tension water is considered as the water closely bound to soil particles. Generally, first the tension water requirements are fulfilled before water is entering the free-water storage, although some important exceptions are present.

2.2.3.1 Upper Zone

The upper zone tension represents the perception volume required under dry conditions"

- To meet all interceptions, and
- To provide sufficient moisture to the upper soil so that percolation can begin.

If the maximum storage capacity of the upper-zone tension is exceeded, water becomes available for the upper zone free-water storage, a temporary storage from which water percolates to the lower zone system and from which water discharges to the channel via the interflow component. The preferred flow direction from the upper zone is the vertical direction, i. e. percolation to the lower zone system.

Interflow occurs only when the precipitation rate exceeds the percolation rate. The upper zone is treated as a linear storage element which is emptied exponentially: discharge = storage X time's storage depletion coefficient. Let the upper zone free-water storage depletion coefficient be denoted by UZK and the upper zone free-water content by UZFWC; then the interflow takes place at a rate:

$$Q_{interflow} = UZFWC*UZK \qquad (2.1)$$

When the perception intensity exceeds the percolation intensity and the maximum interflow drainage capacity, then the upper zone free-water capacity (UZFWM) is completely filled and the excess precipitation causes surface runoff.

2.2.3.2 Lower zone

The lower zone consists of the tension water storage, i.e. the depth of water held by the lower zone soil after wetting and drainage (storage up to field capacity) and two free-water storages: the primary and supplemental storage elements, representing the storages leading to a slow and a fast groundwater flow component respectively. The introduction

of two free lower zone storages is made to have a larger flexibility for reproduction of observed recession curve caused by groundwater flow.

2.2.3.3 Percolation intensity

The percolation rate from the upper zone to the lower zone depends, on the one hand, on the lower zone demand, i.e. requirements determined by the lower zone water content relative to its capacity and, on the other hand, on the upper zone free-water content relative to the capacity. The minimum lower zone percolation demand occurs when all three lower zone storages are completely filled. Then by continuity the percolation rate equals the groundwater flow rate from full primary and supplemental reservoir. Denoting the minimum demand by PBASE then it follows that:

$$PERC_{min.dem} = PBASE = LZFPM * LZPK + LZFSM * LZSK \tag{2.2}$$

Where

LZFPM $\equiv$ lower zone primary free-water storage

LZPK $\equiv$ lower zone supplemental free-water storage capacity

LZFSM $\equiv$ drainage factor of primary storage

LZSK $\equiv$ drainage factor of supplemental storage

The maximum lower zone percolation demand takes place if the lower zone is completely dried i.e if its contentn = 0 then the maximum percolation rate is expressed as a function of PBASE:

$$PERC_{min.dem} = PBASE (1 + ZPERC) \tag{2.3}$$

With ZPERC $\gg$ 1 usually. The actual lower zone percolation demand depends on the lower zone content relative to its capacity. Computationally it means the ZPERC has to be multiplied by a function G of the relative lower zone water content, such that this function:

- Equals 1 in the case of a completely dry lower zone,
- Equals 0 in the case of a completely saturated lower zone
- Represents an approximate exponential decay of the percolation rate in the case of continuous recharge.

In the Sacramento model this function has the following form:

$$G = \left(\frac{\sum \left(\text{Lower zone capacity} - \text{ lower zone content } \right)}{\sum \left(\text{Lower zone capacity } \right)} \right)^{REXP} \tag{2.4}$$

And the actual percolation demand is given by (see also figure 4):

$$PERC_{act.dem.} = PBASE \left(1 + ZPERC * G \right) \tag{2.5}$$

The actual percolation intensity then becomes a function of PERCact.dem. and of the relative upper zone free-water content:

$$PERC = PERC_{act.dem.} * UZFWC/UZFWM \tag{2.6}$$
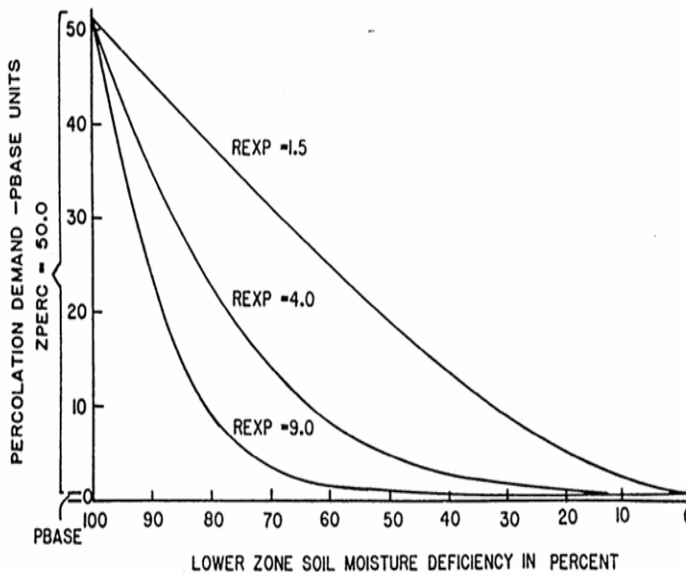
PBASE = the continuing percolation rate under saturated conditions

ZPERC = the number of PBASE units which must be added to the continuing saturated percolation rate to define the maximum percolation condition.

REXP = the exponent which defines the curvature in the percolation curve with changes in the lower zone soil moisture deficiency.

Figure (2.3) Percolation representation curves

2.2.3.4 Distribution of the percolated water

The percolated water drains to three reservoirs, one tension - and two free-water reservoirs. Based on the preceding comments, one would expect that the first the lower zone tension storage is filled up before percolation to the lower zone free water storages takes place. However, variations in soil conditions and in precipitation amounts over the catchments cause deviations from the average conditions. This implies that percolation to the free-water reservoirs, and hence groundwater flow takes place before the tension water reservoir is completely filled.

13

The model allows for this to let a fraction of the infiltrated water percolate to two free-water storages. When the tension water reservoir is full, all percolated water drains to the primary and supplemental free-water storage in a ratio corresponding to their relative deficiencies.

2.2.3.5 Groundwater flow

If the actual contents on the primary and supplemental free-water zones are denoted by LZFPC and LZFSC respectively, then the total base flow QBASE becomes in accordance with the linear reservoir theory:

QBASE =LZFPC * LZPK + LZFSC * LZSK (2.7)

The drainage factors LZPK and LZSK can easily be determined from the recession part of the hydrograph by plotting the part of the hydrograph on semi-logarithmic paper figure (2.4). In the lowest part of the recession curve only the slow base flow component acts whereas in the higher stages both base flow components contribute.

The drainage factor LZPK follows from:

$$K = (QP_t/QP_0)^{1/t}$$ (2.8)

and $$LZPK = 1 - K$$ (2.9)

Where:

K $\equiv$ recession coefficient of primary base flow for the time unit used,

t $\equiv$ number of time units, generally days

QP_0 $\equiv$ a discharge when recession is occurring at the primary base flow rate,

QP_t $\equiv$ t he discharge t time units later.

Let QP_{max} represent the maximum value of the primary base flow, then the maximum water content of the lower zone becomes:

$$LZFPM = QP_{max}/LZPK$$ (2.10)
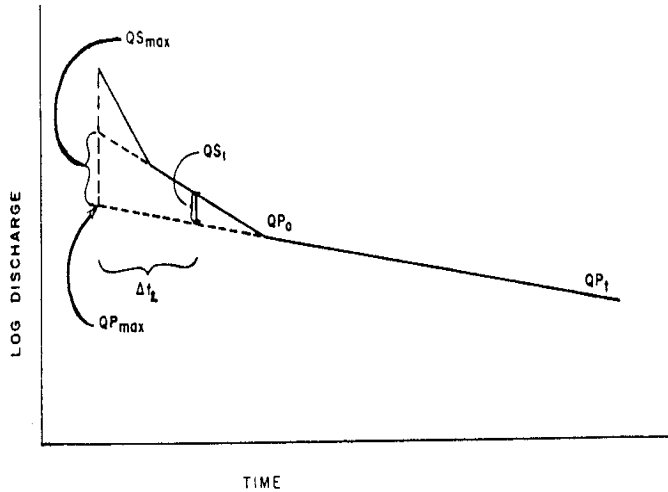
QS$_{max}$ is Lower zone supplemental discharge at time zero.

QS$_1$ is lower zone supplemental discharge arbitrarily used at 2/3 time from peak to QP$_0$.

KS = (QS$_1$/QS$_{max}$)$^{(1/\Delta t)}$ rate of change of supplemental flow.

LZSK = (1-KS) rate of change of supplemental storage

LZFSM = QS$_{max}$/LZSK maximum apparent supplemental storage

Figure (2.4) Definition of recession parameters

And, similarly, the supplemental lower zone free-water capacity is determined; at least this procedure provides first estimates of the lower zone free-water capacities.

The total base flow contributes completely or in part to the channel flow. Complete contribution occurs if subsurface discharge is absent. Otherwise a fraction of the total base flow represents the subsurface flow.

2.2.3.6 Evaporation

Evaporation at a potential rate occurs from that fraction of the basin covered by streams, lakes and riparian vegetation. Evapotranspiration from the remaining part of the catchments is determined by the relative water contents of the tension-water zones. Let ED be the potential evapotranspiration, then the actual evapotranspiration from the upper zone reads:

$$E_1 = ED * (UZTWC/UZTWM) \tag{2.11}$$

i.e the actual rate is a linear function of the relative upper zone water content. In the case E1 < ED water is subtracted from the lower zone as a function of the lower zone tension water content relative to the tension water capacity:

$$E_2 = (ED-E_1) * LZTWC/ (UZTWM+LZTWM) \tag{2.12}$$

If the evapotranspiration should occur at such a rate that the ratio of content to capacity of the free-water reservoirs exceeds the relative tension reservoir content, then water is transferred from free water to tension water, such that the relative loadings balance out.

This correction is made for the upper and lower zone separately. However, a fraction RSERV of the lower zone free water storage is unavailable for transpiration purposes.

2.2.3.7 Impervious and temporary impervious areas

Besides runoff from the pervious area, the channel may be filled by rainwater from the impervious area. With respect to the size of the impervious area, it is noted that in the Sacramento model a distinction is made between permanent and temporary impervious areas where temporary impervious areas are created when all tension-water requirements are met, i.e. an increasing fraction of the catchments assumes characteristics of imperviousness.

2.2.3.8 Routing of the surface runoff

Before the runoff from the impervious areas, the overland – and interflow reach the channel, they may be transformed according to a unit hydrograph leading to an adapted time distribution of these flow rates.

2.2.2.3.9 The channel module

Contributions to the channel flow component are given by:

- Runoff from impervious areas,
- Overland flow from the pervious areas,
- Interflow, and
- Base flow (completely or in part).

The propagation or attenuation of the interflow hydrograph can be described by:

- Summation of outflow from segments,
- Unit hydrograph approach applied to each segment outflow separately,
- A layered routing approach; the inflow hydrograph is divided into a number of layers, where each layer has its own routing coefficient.

2.2.4 Model parameters (Appendix 1)

2.3 Rainfall-runoff model SAMFIL

2.3.1 Introduction

The program SAMFIL has been developed to simulate rainfall-runoff process and to give real-time forecasts of the discharge into rivers due to rainfall on the catchments. Real-time is a key feature of the program.

SAFIL is such model that calculates the discharge into rivers in on-line situation and has data-assimilation option. This means that incoming on-line measurement data can be used to update the model parameters, thereby adapting the model to the actual situation.

The data-assimilation technique implemented in SAMFIL is an Extended Kalman Filter. Actual channel inflow can be used to estimate "state" of the system, consisting of the contents of the conceptual reservoir.

2.3.2 Conceptual model

For use with an Extended Kalman Filter the Sacramento model has slightly been adapted:

- A nonlinear approximation of the discontinuous reservoir outflow
- Evapotranspiration only from the tension–water zones (not from free-water zones)
- No balancing of the relative loadings of the free-water reservoir content with the tension-water reservoir content (in both upper zone and lower zone).

2.3.3 Threshold approximation

Characteristic to the Sacramento model is that it represents outflow from the upper and lower zone reservoirs as a discontinuous function of its contents. E.g. the upper zone tension-water reservoir produces zero outflows until its contents reach its capacity. Once full, the reservoir output is equal to its net input. The threshold-type behavior of the reservoir outflow is substituted by a non-linear reservoir response, and its outflow depends on the degree of saturation.

If the outflow function of the reservoir for a non-negative input u_o, dented by $g(x/x^o, u_o)$. Then the $g(x/x^o, u_o)$ is given by:

$$g\left(\frac{x}{x^o}, u_o\right) = \begin{cases} -u_o & \text{if} \dfrac{x}{x^o} = 1 \\ 0 & \text{otherwise} \end{cases} \qquad (2.13)$$

Figure (2.5) outflow $g(x/x^o, u_o)$ from a Threshold-type reservoir with normalized with content (a/x_o) and input u_o
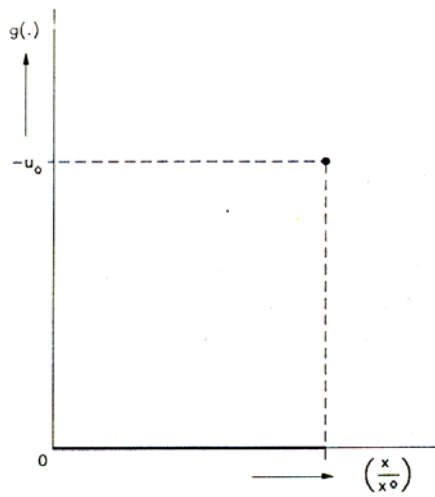
Figure(2.6) outflow $g(x/x^o, u_o)$ from a non-linear reservoir of exponent m, normalized content (a/x_o) and input u_o
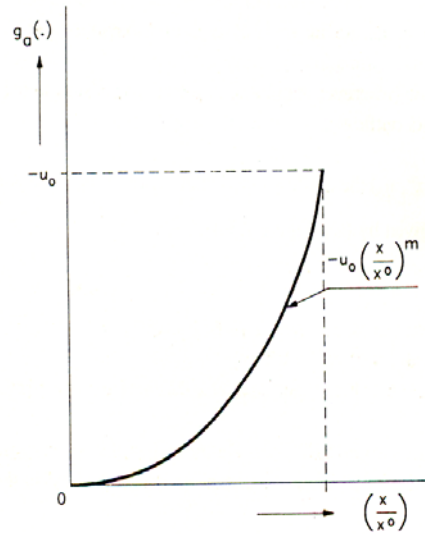
The approximation in Figure (2.6) is used instead of equation (13) and is given by:

$$g_a\left(\frac{x}{x^o}, u_o\right) = -u_o\left(\frac{x}{x^o}\right)^m \qquad (2.14)$$

The higher the value of m the closer $g_a(x/x^o, u_o)$ approximates $g(x/x^o, u_o)$. The domain of definition of x for the approximation is still the closed interval [0, xo]

2.3.4 Catchments parameters in SAMO and SAMFIL
The catchments parameters used by SAMO and SAMFIL represent the same physical quantities however; some SAMO parameters are not used by SAMFIL.

Since SAMO runs with intervals of 1 day and SAMFIL with intervals of 1 hour, the recession parameters UZK, LZPK and LZSK are adapted as follows. Let the recession parameters in SAMO be denoted by X and in SAMFIL by Y, then:

$$Y = -\ln(1-X)/24 \tag{2.15}$$

Where: UZK = the upper zone lateral drainage rate (daily withdrawal to the available content), LZPK = lateral drainage rate of the lower zone primary free water reservoir, LZSK = lateral drainage rate of the lower zone supplemental free water reservoir.

2.3.5 Predication of rainfall from Cold Cloud Duration data

A linear relationship between rainfall and Cold Cloud Duration (CCD) data is assumed as follows:

$$\text{Rain} = f_a.A + B.CCD \tag{2.16}$$

Where:

f_a = fraction of the area covered by cold cloud [-]

A = amount of rainfall [mm]

B = amount of rain per hour of cold cloud coverage [mm/hour]

If runoff is forecast from Could Cloud Duration data, the expression in the equation above substitutes precipitation. The above parameter B is embedded in the Kalman filter.

2.4 Reservoir modules

The FEWS allows testing various reservoir operation strategies before starting forecasting run with the NETFILL model, viz. for the following reservoir:

- Khasham el Girba
- Roseires
- Sennar

This facility will be of particular importance during extreme floods. Various operation schemes can be tested to determine which operation produces the lowest d/s maximum flows, for example a reduction of reservoir levels prior to the arrival of peak flows, which are known some days in advance.

Two dedicated reservoir modules are incorporated, one for the Khashm el Girba reservoir and one for the joint operation of the other two reservoirs. The final results are 10-day

series of required reservoir releases for the next forecasting period. Which are supplied to the NETFIL model as internal boundary conditions. Hence, in NETFIL the structure for the dams reads simply:

$$Q = Q(t) \tag{2.17}$$

No other structure conditions are included in the NETFIL model. All physical limitations, such as maximum possible flow, maximum or minimum possible levels are accounted for in the reservoir module.

In addition lateral off-takes from the reservoirs have to be specified.

Note in that for the updating of the model also only observed reservoir releases and off-takes are used as internal boundary conditions (structure equations). These must be supplied by the user before any update run can start. It is then necessary to check whether the given release flow is indeed less than the maximum possible flow as a function of the level u/s of the dam, viz.:

$$Q \leq Q_{max}(H_{up}) \tag{2.18}$$

The user must select whether he wishes to use the dry season or the wet season reservoir operation procedure for the next forecast for the coming period of 10 days. The starting dates of each season are decided upon by the user.

2.5 River flow modeling (Flow routing model NETFIL)

The program NETFIL has been developed to calculate water levels and flow in an open channel network containing structures (like weirs and sluices) in real time. This real-time aspect is a key feature.

The dynamical model incorporated in NETFIL is described by the complete St. Venant equations for non – steady flow. Structures are described by special equations. Boundary conditions and lateral flows are defined by time-series of water flows.

Calculations of unsteady flow in open channel networks have been and will be performed in numerous cases for design purposes or scenario evaluation .these concern off-line activities. DELFT HYDRAULICS has applied the program WAFLOW (part of the WENDY system) to this end in large number of studies.

If calculations for unsteady flow are required in an on-line situation a program must be applied containing data-assimilation option. This means that incoming on-line water level

measurement data can be used to update the model parameters, herewith adapting the model to the actual situation. NETFIL is such model. The data-assimilation technique implemented in NETFIL is an extended Kalaman Filter. Actual water level data can be used to estimate the "state" of the model, consisting of water level, flows, bottom roughness factors and global wind stress coefficient.

2.5.1 Flow equations

WAFLOW is a one-dimensional dynamic flow model, based on the full Saint-Venant equations for unsteady flow. The Saint-Venant equations consist of a continuity equation and a momentum equation.

Continuity Equation:

$$\frac{\partial As}{\partial t} + \frac{\partial Q}{\partial x} - ql = 0 \qquad (2.19)$$

Momentum equation;

$$\frac{\partial Q}{\partial t} + \frac{\partial}{\partial x}\left(\alpha \frac{Q^2}{A_f}\right) + gA_f \frac{\partial H}{\partial x} + g\frac{Q|Q|}{C^2 RA_f} - B_f \frac{\tau_\omega}{\rho_\omega} + gA_f \eta = 0 \qquad (2.20)$$

In which

A_f	=	flow conveying area of cross-section	(m^2)
A_S	=	total cross-sectional area (including storage)	(m^2)
B_f	=	flow width	(m)
C	=	Chèzy coefficient for hydraulic roughness	$(m^{1/2}/s)$
g	=	acceleration due to gravity	(m/s^2)
H	=	water level	(m)
Q	=	discharge	(m^3/s)
q_l	=	lateral discharge per unit length	(m^2/s)
R	=	hydraulic radius	(m)
t	=	time	(s)
x	=	length coordinate along branch	(m)
α	=	reduction coefficient accounting for the non-uniform velocity distribution in a cross-section with respect to momentum convection	$(-)$

η =   head loss per unit length due to additional resistance   (-)

ρ_w =   density of water (kg/m^3)

τ_w =   wind shear stress   (Pa)

The equations account for the effects of inertia, convection, pressure graduations, bottom shear stresses, wind shear stresses, additional resistance and lateral discharges.

2.5.2 Boundary conditions

The following boundary conditions can be specified at the upstream and downstream ends of the network:

- The water level as a constant or as a function of time (a weir or a spillway can be incorporated),
- The discharge as a constant or as a function of time,
- A rating curve, either by specifying water level as a function of discharge or discharge as function of water level.

Lateral discharge can be specified as "internal boundary conditions" (sources and sinks). They can be constant or function of time.

2.5.3 Cross-sections

The schematization of a cross-section in WAFLOW is depicted in Figure (2.7) two distinctions can be made.

The first distinction is one between flow area and storage area. Water in the the storage area dose not contribute to the flow capacity of the channel. It can is only stored or released when the water level in the cross-section varies.

The second distinction compromises the division of the flow area into one, two or three sub-areas. For each sub-area, a different hydraulic roughness can be specified. Thus the main channel and flood plains may be combined into one composite cross-section with different average flow velocities per sub-area.

Figure (2.7) Definition of cross-section in WAFLOW
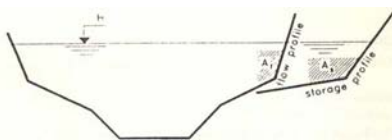
2.5.4 Hydraulic roughness

The flowing options for specifying the hydraulic roughness are available:

- Chèzy coefficient specified directly,
- Chèzy coefficient calculated according to White-Colebrook:

$$C = 18\log\frac{12R}{k_s} \tag{2.21}$$

In which k_s denote the equivalent sand roughness according to Nikuradse.

- Chèzy coefficient calculated according to Manning-Strickler:

$$C = kR^{1/6} \tag{2.22}$$

In which k denote the reciprocal of the Manning roughness coefficient.

- Chèzy coefficient calculated with roughness predictor in which the Chèzy coefficient is a function of the Shields parameter.

2.5.5 Structures

Regulators, Spillways, weirs, sluices, barrages, bridge piers, abutments, open flumes and culverts can be specified. Options for structures maintaining a constant head loss or a constant discharge are also available. It is possible to specify variation in time of valves, gate positions, sill heights, etc.

2.5.6 Additional resistance

Additional resistance can be specified. In this way, local head losses in open channel can be incorporated.

2.5.7 Wind

The shear stresses on the water surface due to wind forces can be incorporated in WAFLOW. The direction and the force of the wind can be defined as function of time.

2.5.8 Numerical solution

The numerical model is based on an implicit staggered-grid solution method (Crank-Nicholson). The non-linear flow equations are linearized with respect to the values of Q and H at a previous time step or a previous iteration step.

2.5.9 Model accuracy

The accuracy of the computational results depends on a number of factors, viz:

- The assumptions made in the mathematical model,
- The schematization of the model,
- The availability and quality of the input data, and
- The numerical parameters.

2.5.10 Data assimilation

The forecasts of water levels and discharges in the river network are based on a dynamic model and on real-time observations. The dynamic model is based on physical knowledge of the river network. The best forecast is obtained if the information from both the dynamic model and the observation is integrated in such a way that the resulting estimate has minimum uncertainty. This can be done by data assimilation. The NETFIL system for data assimilation consists of the dynamic flow model component WAFLOW and a component for the processing of measured water levels, i.e the Extended Kalman Filter (EKF). In Kalman filtering terminology, the flow model component is called the "state equation" which is solved in the "time update", and the measured water levels processing component is called the "observation equation" which is solved in the "measurement update".

The state equation is used to forecast the future state of the river network. Each time when measurements are collected, the forecast values are compared and adjusted to them. The degree of adjustment depends on the build-in estimates of the uncertainties of the dynamic model ('system noise') and the uncertainties of the observations ('measurement noise').

The time update and the measurement update are applied alternately. In each computation step, first the time update is executed, then the measurement update. If no measurements

are available in a computation step, the results of the measurement update are kept identical to the results of the time update.

The difference between the Extended Kalman Filter (EKF) used in NETFIL and ordinary linear Kalman filter is that EKF can handle nonlinear equations as well. The nonlinear equations are then linearized about the current best estimate of the actual state.

2.6 The Kalman-filter

2.6.1 Introduction

One often has two base of information which enables the forecasting of river flows, viz.:

1. Observation in the river basin

Observations will contain uncertainties. Sensors cannot provide perfect and complete data about the basin because not all desired variables can measure (i.e. spatial variability in rainfall) and measurements are usually noise corrupted.

2. A mathematical model of the river basin

Mathematical models, based on physical knowledge of the river basin represent key aspects of the behavior of the river basin. However, even the most sophisticated (mathematical) model of the river basin contains uncertainties

2.6.2 Dynamic system

Kalman filters are applied to estimate the "state" of a dynamic system. A dynamic system can be represented in the so-called state space form, consisting of two equations:

$$X(t+1) \quad = \quad F.X(t) + G.W(t) + C.U(t) \tag{2.23}$$

$$Y(t) \quad = \quad H.X(t) + V(t) \tag{2.24}$$

With

$X(t)$	$\equiv$	state vector
$W(t)$	$\equiv$	system noise
$U(t)$	$\equiv$	input vector
$Y(t)$	$\equiv$	observation vector
$V(t)$	$\equiv$	measurement noise
F, G, C, H	$\equiv$	matrices with constant coefficients
t	$\equiv$	time

The system is characterized by its "state", represented in the vector X (t). The vector X (t+1) is determined by X (t), the (known) input vector U (t) and the (unknown) "model error" or system noise" vector W (t).

The equations (21) and (22) are linear difference equations. Linearity is not essential for state space formulations.

Difference equations correspond to a discrete-time representation of the system. Continuous-time representations with differential equations are also possible.

Important assumptions on the stochastic characteristic of the noise are that the covariance matrices of the initial condition, the system noise and the measurement noise are mutually independent.

Let P (0) = E X (0) X (0) ^{T}, Q = E W (t) W (t) ^{T}, respectively. R = E V (t) V (t) ^{T} denote this covariance matrices. Then the mutual independence implies the following:

E X (0) W (t) ^{T} = 0

E X (0) V (t) ^{T} = 0

E W (t) V (t) ^{T} = 0

V (t) and W (t) are independent identically distributed Gaussian process.

2.6.3 Linear Kalman Filter

With the assumption of the previous section it is possible to derive an estimator of X (t) with following properties:

- Linearity

- unbiasedness

- optimality in least squares sense

This estimator is given by the Kalman Filter algorithm:

$$X^{\wedge} (t + 1 \mid t) = F. X^{\wedge} (t \mid t) + C.U (t) \tag{2.25}$$

$$X^{\wedge} (t + 1 \mid t+1) = X^{\wedge} (t +1 \mid t) + K (t +1) [Y (t +1) - H. X^{\wedge} (t +1 \mid t)] \tag{2.26}$$

$$P (t+1 \mid t) \quad = F.P (t \mid t) F^T + G.Q.G^T \tag{2.27}$$

$$P (t+1 \mid t +1) = P (t +1 \mid t) - P (t +1 \mid t).H^T. [H.P (t +1 \mid t). H^T + R]^{-1} .H.P (t +1 \mid t) \tag{2.28}$$

$$K (t+1) = P (t+1 \mid t) .H^T [H.P (t+1 \mid t) H^T+R]^{-1} \tag{2.29}$$

$$X^{\wedge} (0 \mid 0) \quad = X_0$$

$$P (0 \mid 0) \quad = P_0$$

The matrix $P(.|.)$ can be interpreted as the covariance matrix of $X^{\wedge}(.|.)$. Equations (2.27) – (2.29) can be applied off-line without using any measurement data, resulting in a convergence of $K(t)$ to the steady state Kalman gain $K\infty$.

2.6.4 Nonlinear Kalman Filter, EKF

The algorithm of section 2.6.3 is applicable to linear systems. Now we study a nonlinear system.

$$X(t+1) = f(X(t), U(t) + G(t).W(t) \tag{2.30}$$
$$Y(t) = h(X(t)) + V(t) \tag{2.31}$$

By linearizing equations (2.28) and (2.29) every time-step a spatial form of the Kalman Filter algorithm, referred to as Extended Kalman Filter, can be derived. In some cases measures must be taken to prevent filter divergence.

A steady-state Kalman gain $K\infty$ does not exist and equations (2.25)-(2.27) must be evaluated every time-step.

Using the notation

$$F_t = \partial f/\partial X \big| x = X^{\wedge}_{t|t} \qquad H_t = \partial h/\partial x \big| x = X^{\wedge}_{t|t-1} \qquad G_t = \partial G/\partial x \big| x = X^{\wedge}_{t|t}$$

The algorithm consists of:

$$X^{\wedge}(t+1 | t) = f(X^{\wedge}(t | t) + U(t)) \tag{2.32}$$
$$X^{\wedge}(t+1 | t+1) = X^{\wedge}(t+1 | t) + K(t+1)[Y(t+1) - h(X^{\wedge}(t+1 | t))] \tag{2.33}$$
$$P(t+1 | t) = F_t P(t | t) F_t^T + G_t Q G_t^T \tag{2.34}$$
$$P(t+1 | t+1) = P(t+1 | t) - P(t+1 | t)H^T_{t+1}[H^T_{t+1}P(t+1 | t)H^T_{t+1} + R]^{-1} H_{t+1}P(t+1 | t) \tag{2.35}$$
$$K(t+1) = P(t+1 | t) H^T_{t+1} [H_{t+1}P(t+1 | t) H^T_{t+1} + R]^{-1} \tag{2.36}$$

Equations (32) and (34) together are called the "prediction step"; equations (2.33), (2.36) and (2.36) are called the "filter step".

2.6.5 Parameter estimation with the Kalman filter

Consider the linear system

$$X(t+1) = F(\alpha) X(t) + C(\alpha) U(t) + GW(t) \tag{2.37}$$
$$Y(t) = H(\alpha) X(t) + V(t) \tag{2.38}$$

The matrices F (α), C (α) and H (α) depend on parameter α in an arbitrary way. It is assumed that all elements are of these matrices are differentiable with respect to α. Considering it as an additional state in an augmented system

Define the augmented state vector:

$$X_a(t) = \begin{pmatrix} X(t) \\ \propto(t) \end{pmatrix} \tag{2.39}$$

The α(t) = α for all t. We now have the flowing state equations:

$$X_a(t+1) = \begin{pmatrix} F(\propto)X(t) + C(\propto)U(t) + GW(t) \\ \propto(t) \end{pmatrix} \tag{2.40}$$

$$Y(t) = H(α)X(t) + V(t) \tag{2.41}$$

We can apply the EKF algorithm to these equations to obtain an estimate of α(t). We assume that   α(t) is not affected by noise so that the system noise matrix for the augmented system has the following form:

$$Q_a = \begin{pmatrix} Q & 0 \\ 0 & 0 \end{pmatrix} \tag{2.42}$$

We may initialize as follows.

$$X\hat{}_a (0 \mid 0) = \begin{pmatrix} X\hat{}a (0 \mid 0) \\ \propto\hat{}(0) \end{pmatrix} \tag{2.41}$$

$$P_a (0 \mid 0) = \begin{pmatrix} P (0 \mid 0) & 0 \\ 0 & \sum(0) \end{pmatrix} \tag{2.44}$$

Where $\sum(0)$ represents some a-priori information about α.

2.7 Regression models

Multiple regression equations were established for the Rahad and Dinder catchements for runoff prediction. The models are of the type:

$$Q_X(t) = f(P_X(t), P_X(t-1), Q_X(t-1), Q_Y(t)) \tag{2.45}$$

Where:

$Q_X(t)$ = runoff from catchment X (= Rahad or Dinder) on day t

$P_X(t)$ = rainfall in catchement X on day t

$P_X(t-1)$ = rainfall in catchement X on day t-1

$Q_X(t-1)$ = runoff from catchment X on day t-1

$Q_Y(t)$ = runoff from Blue Nile catchement at Eddeim on day t

2.8 Simple Non –Storage Routing

This is a very approximate method, but since there are no significant lateral inflows between the stations the method was used.

The station is:

$$H_D = AH_U + G \tag{2.46}$$

H_D & H_U where stage for downstream and upstream respectively and A & G are constant

Chapter Three
Materials and Method

3.0 Introduction

This chapter will discuss the materials and methods used in this study. The estimation of rainfall over Ethiopian plateau is also discussed. Flow data availability is also over viewed a long with preprocessing.

3.1 Rainfall estimate

The rainfall over the Ethiopian catchment is estimated using remote sensing information, catchment viz.a.viz Cold Cloud Duration (CCD).

The rainfall-runoff models were calibrated using Cold Cloud Duration data derived from Meteosat TIR image available in the archive of the TAMSAT group of Reading University for the 1987, 1988, 1989, and 1990 flood season.

3.1.1 Estimates of the Cold Cloud Duration (CCD)

The TAMSAT group at Readding University has prepared the software package ARCS for the extraction of Cold Cloud statistics from Meteosat TIR images, for up to 15 sub-catchments. ARCS is acronym for Area Rainfall and Cloud Statistic.

Because the system does not work, another method of obtaining CCD & Cold Cloud Cover (CCC) from internet for the year 2003 up to 2007 was used. This is done as follows:

Go to website   ftp://edcftp.cr.usgs.gov/pub/edcuser/fewsips/africa/

1. Copy the files of rainfall for examples it look like this **rain_20083.tar** (it read the rainfall on the 3rd day in 2008) days in digital from 1 to 365.

2. Convert the above file to the text by Narcs2 software working under DOS environment for example C:\ Document and settings\ Desktop\ NARCS2\ **narcs2all rain_20083***

3. In the same directory   you find files of type Notepad named blunile, settit, kubor, dinder and rahad. Inside each written the name of the file entered and N1 and N2 e.g (rain_20083   N1   N2) $\equiv$ (rain_20083   2.581   0.051).

4. CCC = N2 (0.051) without percentage (for FEWS multiply by 100), $CCD = N2(0.051 - \dfrac{A}{100})$, A from table 3.2

The CCD data will be entered directly to the hydrological models and conversion to catchments rainfall estimates will take place within the model.

3.1.2 Rainfall-CCD estimation parameters

To account for spatial homogeneity in rainfall in the development of rainfall-runoff models for the Blue Nile, Rahad, Dinder and Atbara basins a total of 9 sub-catchment areas have been discerned, see Table 3.1:

(Table 3.1 Summary of sub-catchments for CCD-parameter estimation)

River	Sub-Catchments nr	Sub-Catchments name	Total area of catchments in Km^2
Blue Nile	1	Lake Tana and Abbai up to Agibar	
	2	Middle Abbai up to Didessa Confluence	
	3	Didessa River Basin	
	4	Abbai with Dibus and Balas up to Eddeim	324,530
Dinder	5	Dinder river Basin (16,000 km^2)	
Rahad	6	Rahad River Basin	
Atbara u/s	7	Atbara u/s of setit confluence	
Atbara Setit	8	Uper Tacazze river Basin (40,585 km^2)	112,000
	9	Lower Tacazze river Basin (28,797 km^2)	

For each of these sub-catchments daily CCC (Cold Cloud coverage) and CCD data of the years 1987-1990 at least for the months July to September were prepared from the TAMSAT-archive. To arrive at rainfall data the parameters of the rainfall-CCD relation were estimated in principle for each sub-catchment. However, some clustering of catchments was necessary due to non-availability of point rainfall measurements in some of the catchments.

For each catchments two sets of calibration parameters have been produced based on two different data treatment methods. In both methods, the first stage is to define a cloud to temperature threshold below which the cloud may be designated as "rain-bearing". This is done by comparing the presence or absence of rain in a rain-gauge on a given day with the presence or absence of cold cloud below the temperature threshold for the pixel

31

corresponding to the rain gauge. The selected temperature threshold is the one with the highest score of rain/no-rain predictions over the region.

Having established a temperature threshold, a linear regression is performed to establish the relationship between rainfall quantity and the number of hours of cloud below the threshold. Two calculations have been done. In one, Method 1, the regression is based on sorting the rain-days into classes based on the CCD and using the median rain in each class as a regression variable. In the other, Method 2, mean rain per rain-day is regressed against mean CCD. Table 3.2 shows the rainfall parameters obtained.

(Table 3.2 Rainfall estimation parameters)

Catchments	Method 1						Method 2						CCD Tem.
	July		August		September		July		August		September		
	A	B	A	B	A	B	A	B	A	B	A	B	
Kubur & Helow	2.3	1.2	2.5	1.7	-1.3	1.3	7	1.1	4.8	1.6	2.3	0.8	-40°C
Blue Nile	4	1	4	1	3	0.9	7	1.1	7	1.2	6	0.9	
Dinder & Rahad	-1.55	2.17	-3	2.9	-4.4	2.3	15.3	-1.1	9.3	0.7	11.8	-0.4	-60°C

The Equation of rainfall is: Rainfall (mm) $= A * \dfrac{CCC}{100} + B*(meanCCD)$

In Table 3.3 a comparison is presented between the two parameter estimation procedures based on monthly average rainfall for the period 1987-1990, Derived from CCD

(Table 3.3 a comparison between methods (Rainfall monthly total in mm))

	Method 1			Method 2			Method 1/ Method 2		
Catchment	Jul	Aug	Sep	Jul	Aug	Sep	Jul	Aug	Sep
1	248	196	75	310	260	110	0.80	0.75	0.68
2	193	195	97	247	251	153	0.78	0.78	0.63
3	180	179	207	259	274	300	0.69	0.65	0.69
4	237	194	156	331	280	262	0.71	0.69	0.60
1-4*	215	193	120	283	263	187	0.76	0.73	0.64
1-4**	209	190	122	280	262	179	0.75	0.73	0.68
5	72	71	36	165	161	148	0.44	0.44	0.24
6	69	81	32	156	157	121	0.44	0.51	0.26
7	224	290	106	330	339	136	0.68	0.85	0.79
8-9	143	192	406	229	235	70	0.62	0.82	0.66

Notes   1: rainfall values in mm
         2:   * = derived from sub-catchment averaged rainfall

              ** = derived from sub-catchment averaged parameters

Table 3.3 shows that Method 2 produces consistently higher rainfall estimates, considerable difference in rainfall is observed for the catchments numbers 5 and 6 (Dinder and Rhahad), because of the poor quality of rainfall data for these catchments.

The point rainfall data is insufficient to compute reliable catchment rainfall figures, so no definite answer can be given as to the most appropriate method. However, water balance calculations indicate that Method 2 gives likely too high values. For example, for the Blue Nile basin the sum of potential evapotranspiration and runoff from July to September (average of years 1987-1990) amounts to 460 mm, the basin conditions on 1 July and 30 September will not differ very much, this amount should approximately balance with the rainfall. The average rainfall during the same period according to method 1 and method 2 is respectively 538 mm and 733 mm. so, whereas Method 1 gives an approximately closed water balance (surplus of 78 mm), Method 2 leads to an unrealistic high balance-surplus of 273 mm. Therefore, for the calibration of the rainfall-runoff models use have been made of the rainfall estimates derived with Method 1.

3.2 Evapotranspiration

The potential evapotranspiration in the Blue Nile basin was derived from the records of Addis Ababa, Lake Tana and Roseires, given by Shahin in (1985). Table 3.4 shows the adopted values as presented in the rightmost column of this table.

(Table 3.4 monthly evaporation in and around the Blue nile basin and Atbara basin)

Month	Evaporation in mm/day						
	Atbara Basin			Blue Nile Basin			
	Kassala	L.Tana	Atbara	Addis A.	Roseires	L.Tana	B.Nile
July	4.3	1.1	2.2	4.2	5.0	1.1	3.1
August	3.3	1.1	3.0	4.1	5.1	1.1	2.4
September	3.3	1.4	3.5	4.7	5.3	1.4	3.8

3.3 Runoff

Meteorological data available based on the Cold Cloud Cover (CCD) - derived catchments rainfall data (period July to September) for years 1987-1992 and lately for year 2007.

Hydrological database of available water level data on daily base for the Eddeim, Khartoum and Dongola are from 1985 –to date. Available stage-discharge data for Eddeim last one is in the year 1992, Khartoum is for years 1985-1994 in the flood period it takes at Soba with very rare at peak of flood, for Dongola is available for years 1985-to date the available data used in FEWS including cross sections.

3.3.1 Blue Nile

To minimize differences between observed and simulated streamflows, calibration process was carried for estimation of model parameter values.

Runoff data are only available for the gauging station Eddeim, i.e. at the outlet of the basin. No outflow data were available for the identified sub-basin. The basin outflow was derived from recorded daily water levels at Eddeim and the stage-discharge relation presented in equation $Q = 99.43(H-5.39)^{2.024}$, $(7.5<H<14.5$ m) Q and H are discharge and stage respectively.

Blue Nile was divided to four segments, and calibration carried for one segment, with catchment area of 179486 km^2, applying an average time shift of 3 days to the rainfall to account for the travel time to Eddeim.

The adopted parameter set for one-segment approach is presented in table 3.5

(Table 3.5:SAMO parameters for the Blue Nile basin (for more details see appendix 1))

Parameter	Value	Parameter	Value
UZTW	50 mm	ZPERC	75
UZFW	40 mm	REXP	1.0
LZTW	230 mm	PFREE	0.5
LZSFW	25 mm	SIDE	0.0
LZFPW	100 mm	PCTIM	0.05
UZK	0.125 fract./day	SDIMP	0.0
LZSK	0.030 fract./day	SARVA	0.0
LZPK	0.017 fract./day	SSOUT	0.0 mm/day

3.3.2 Dinder upstream of Gwasi and Rahad upstream of Hawata relative to B. Nile

The daily flows of the Dinder and the Rahad rivers shows a high auto-correlation. The models adopted are of the form of equation (2.45). Temporarily, the variables Px(t), Px(t-1) were left out of the relation because of the poor quality of rainfall data for these catchments. The following equations were established:

For the Dinder river at Gwasi:

$Q_t = 0.868*Q_{t-1} + 0.0088*Q_{t,Eddeim}-1.2 \ m^3/s$.

For the Rahad river at Hwata:

$Q_t = 0.831*Q_{t-1} + 0.0048*Q_{t,Eddeim}-.8 \ m^3/s$. Where Q is discharge and t is time in day

3.3.3 Setit upstream of wad el Heleiw

Runoff data are only available for the gauging station Wad el Heleiw. The discharge at Wad el Heleiw was derived from recorded daily water levels and the stage-discharge relation presented in equation $Q = 380.2*(H-7.97)^{1.404}$ for 8.49 <H <15 m Q&H discharge and stage respectively.

Similar To Blue Nile Setit Basin was calibrated as one segment as Tacazze catchment area 40585 km^2, Appling an average time shift of 1 day to the rainfall, to account for travel time to Wad el Heleiw. Table 3.6 shows SAMO parameters for the for the Setiet Basin and Kubur basin.

(Table 3.6: SAMO parameters for the for the Setiet Basin and Kubur basin)

Parameter	Value	Parameter	Value
UZTW	100 mm	ZPERC	50
UZFW	40 mm	REXP	2
LZTW	230 mm	PFREE	0.5
LZSFW	30 mm	SIDE	0.3
LZFPW	100 mm	PCTIM	0.03
UZK	0.125 fract./day	SDIMP	0.12
LZSK	0.090 fract./day	SARVA	0.03
LZPK	0.020 fract./day	SSOUT	0.0 mm/day

The initial reservoir contents used in the calibration years are summarized in table 3.7

(Table 3.7: Initial reservoir contents in (mm))

Initial	Blue Nile SAMO model					Setit SAMO model				
Capacity	UZTW	UZFW	LZTW	LZFSW	LZFPW	UZTW	UZFW	LZTW	LZFSW	LZFPW
	50	40	230	25	100	130	30	130	30	60
1987	50	0	210	5	15	65	0	110	2	5
1988	45	0	220	5	20	95	0	220	2	5
1989	35	0	175	3	15	70	0	120	1	3
1990	40	0	200	2	10	80	0	210	1	4

3.4 Flood Routing

3.4.1 NetFill model

NetFill model computes water levels and discharge in an open-channel network with structure in real time. It consists of a dynamic flow model component, WAFLOW, and a data assimilation component. The latter adapts the model to the actual situation by updating the model parameters on the basis of incoming water level measurement data. The process is going through branches and nodes and takes cross-sections (H-point) for interpretation and prediction of water level and discharge after entering boundary conditions.

3.4.1.1 lay-out of cross-section (H-point)

The Details on branches, structures and boundary conditions are given in

Tables 3.8 (A and B)

(Table 3.8 (A): structure of the model Branches)

Name	Branch number	Upstream node number	Downstream node number	Branch length[km]	Number of H-point (x-section)
Blue Nile	1	0	1	108.2	7
	2	1	2	187.3	13
	3	2	19	86.0	7
	28	19	3	1.0	3
	4	3	4	93.8	7
	5	4	5	61.0	5
	6	5	8	191.3	12
Off-takes wad Alais	21	0	2	0.01	3

Off-takes Gezira & Managil	22	0	19	0.01	3
Dinder	23	0	4	0.01	3
Rahad	24	0	5	0.01	3
White Nile	7	0	6	32	17
	9	6	7	6	4
	8	7	8	6	4
White Nile pumps schemes	27	0	6	0.01	3
Atbara	25	0	20	60.0	8
	29	20	18	1.0	3
	10	18	11	435.0	10
Girba Main canal	26	0	20	0.01	3
Main Nile	11	8	9	65.0	5
	12	9	10	137.0	9
	13	10	11	119.5	8
	14	11	12	87.0	6
	15	12	13	136.5	9
	16	13	14	124.0	7
	17	14	15	79.5	5
	18	15	16	111.0	7
	19	16	17	111.5	6
	20	17	0	97.5	6

(Table 3.8: B structure of the model reservoir)

Node number	Name	Type
1	Roscires	Dam
3	Sennar	Dam
7	Jebel Aulia	Dam
18	Khashm el Girba	Dam

3.4.1.2 Boundary conditions

Table 3.9 below gives the boundary conditions used in the routing process.

(Table 3.9: boundary conditions for entering data)

Name	Branch Number	Type of conditions	Sign
Blue Nile at Eddeim	1	Q(t)	+
Pump schemes Wad Alais	21	Q(t)	-
Pump schemes Gezira/Managil	22	Q(t)	-
Dinder	23	Q(t)	+
Rahad	24	Q(t)	+
White Nile at Malakal	7	Q(t)	+
White Nile pump schemes	27	Q(t)	-
Atbara: Sum of Kubor and Wad el heleiw	25	Q(t)	+
Girba Main Canal	26	Q(t)	-
Dongola	20	Q(H)	

3.4.2 Simple Non – Storage Routing

Here is a fit of curve to the relationship, to give satisfactory forecasts of the downstream stage from an upstream stage measurement. Table 3.9 shows the equation curve updated day by day in the flood period

(Table 3.9: The equation curve updated day by day in the flood period)

station	Upstream Station	Downstream station	equation curve
Eddeim	Estimated rainfall in Athiopia	Eddeim	$H_D = AH_U + G$ H_D **&** H_U where stage for downstream and upstream respectively and **A** & **G** are constant update day by day
Khartoum	Madani	Khartoum	
Dongola	Marawi	Dongola	

3.4.2.1 Rainfall – Runoff Relationship Method

In study of relation between catchment yields represented by daily values of estimated daily areal rainfall and runoff represented daily stage at Eddeim, a moderate linear relation exists, with equation: Runoff at $Eddeim_{n+3} = 0.0599 \, RFE_n + 10.19$. Figer (3.1)

Figure (3.1a): Comparable Rainfall - Runoff on the River Blue Nile at Eddeim
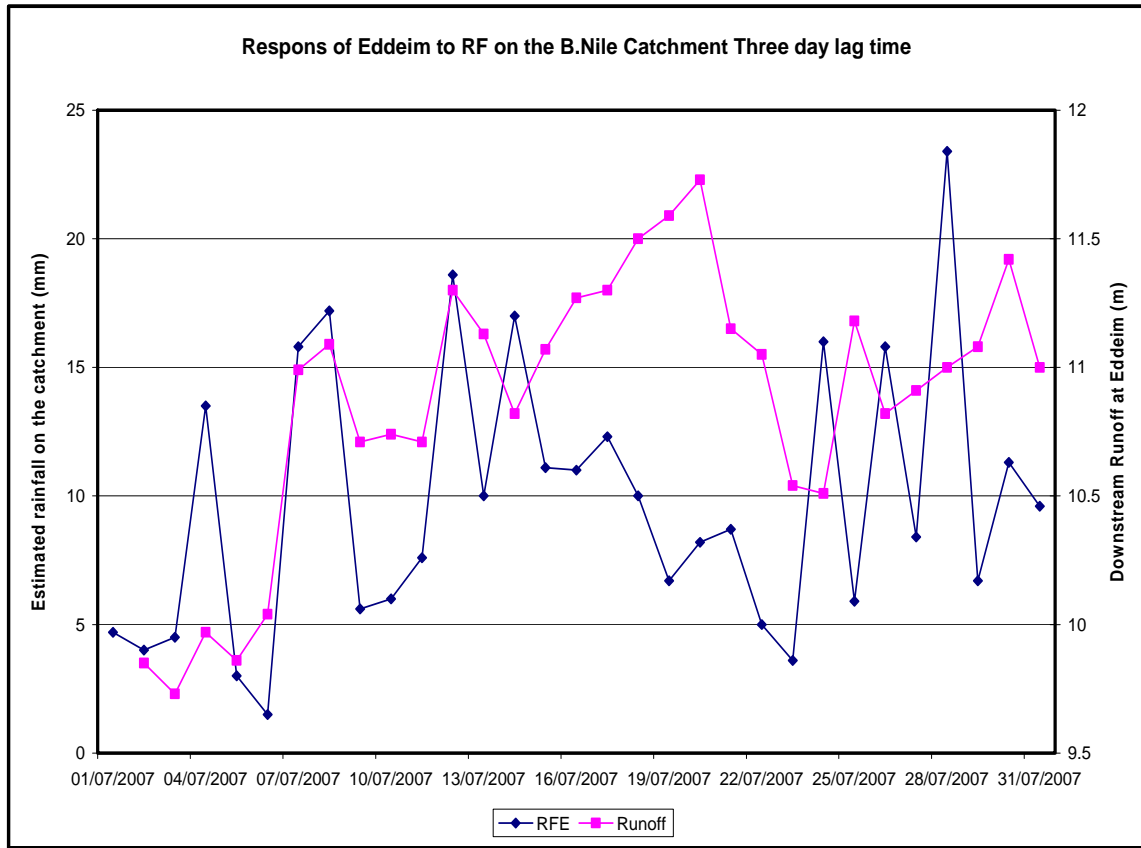

Figure (3.1a) is time series hydrograph and superimposed on it rainfall of Blue Nile catchments three days late. it can be seen that the lead time of rainfall on blue Nile catchments to approach at Eddeim station, three days for the first half of July and second half was found four days to approach at Eddeim staion my be the bushes and grass cover the earth and frequently delay the runoff to approach Eddeim station.

Figure (3.1b): Relation between Rainfall and Runoff at Eddeim

Relation between estimated RFE at Blue nile catchment and runoff at Eddeim station on daily base (1-31) July 2007

Runoff at Eddeim$_{n+3}$ = 0.4126Ln(RFE$_n$) + 9.9877
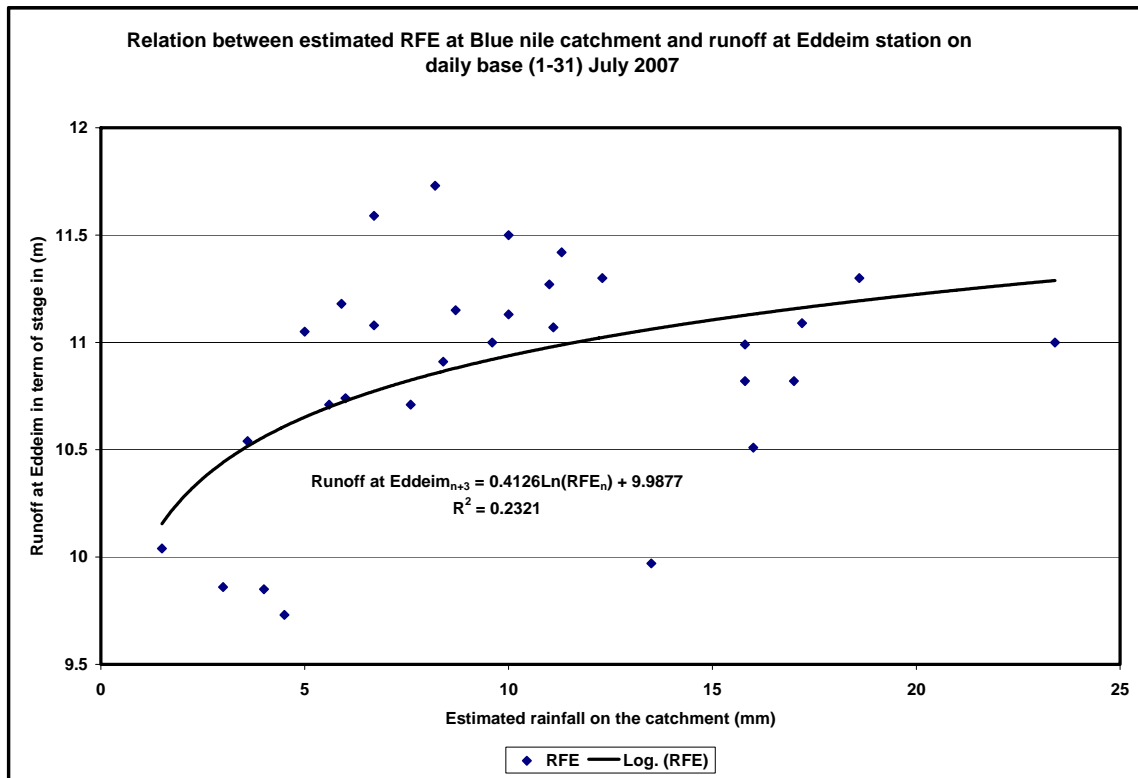R^2 = 0.2321

RFE ——— Log. (RFE)

Figure (4.1b) is correlations between the rainfall at the Blue Nile catchments and runoff at Eddeim station the correlation is found alogarithmic with equation (Runoff at Eddeim$_{n+3}$ =0.4123ln (RFE$_n$) +9.9877) and (R^2 = 0.2321) for the whole period of July. Figures 4.1a and 4.1b, suggests that the rainfalls on Blue Nile catchments are not consistently reliable. This may be because of the systematic error in the changing of RFE parameters or calculations of CCD and CCC by satellite is not correct.

3.4.2.2 Stage-Stage Relationship

A linear relationship exists between daily stages of an upstream gauging station at Wad madani and a station at Khartoum, 202km downstream, 12/1000000 slop. 31 comparable stages (m) for starting flood of 2007 beginning of July are shown in Figure 3.1 an equation   Khartoum Stage (m) $_{n+1}$ = 0.6475Madani stage (m) $_n$ + 3.818 relating Khartoum, the downstream stage to Madani, the upstream stage, giving forecast values of Khartoum stage one day lead time figure (3.2) similarly very high relation between Marwi stage and Dongola stage exist with equation:

$Dongola_{n+1}$ = 0.6916$Marawi_n$ + 1.9374 for the same period Figure (3.3)

Figure 3.2a shows comparable stage-stage on the River Blue Nile at Khartoum

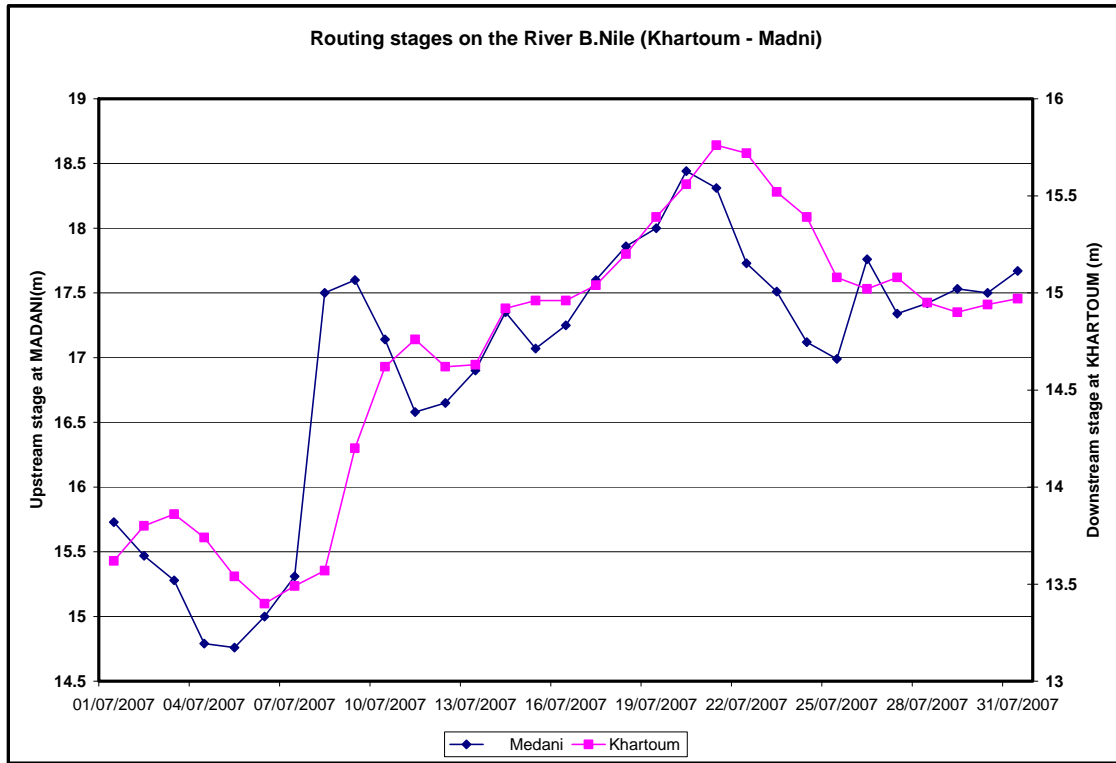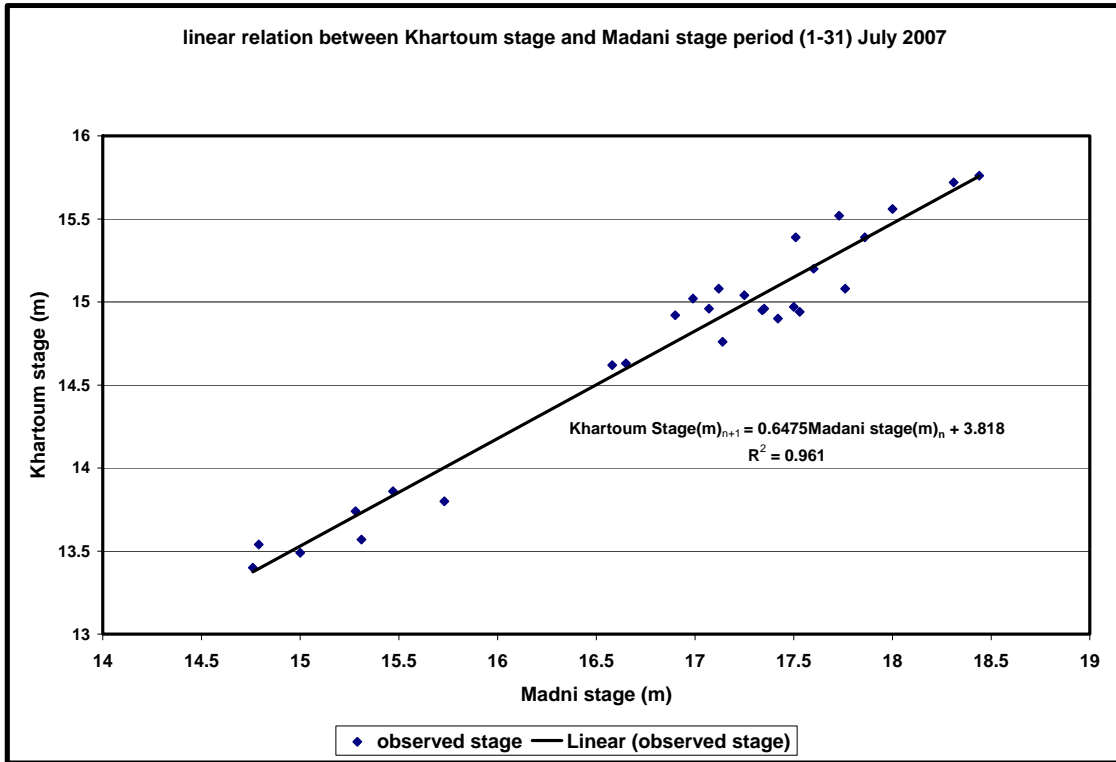**Figure (3.2a): Comparable stage-stage on the River Blue Nile at Khartoum**

Figure 3.2a is time series hydrograph of Madni station and Khartoum station and the data for July 2007. It can be seen one day lead time.

Figure 3.2b shows correlations of stage-stage on the River Blue Nile at Khartoum

Figure (3.2b): Relation between Khartoum stage and Madani stage July 2007

linear relation between Khartoum stage and Madani stage period (1-31) July 2007

Khartoum Stage$(m)_{n+1}$ = 0.6475Madani stage$(m)_n$ + 3.818
R^2 = 0.961

It can be seen in figure 3.2b the correlation between the flows at Madani and Khartoum is high (R^2 = 0.96). This also it shows the good quality of data.

Figure 3.3a comparable stage-stage on the River Blue Nile at Dongola

Figure (3.3a): comparable stage-stage on the Main Nile at Dongola
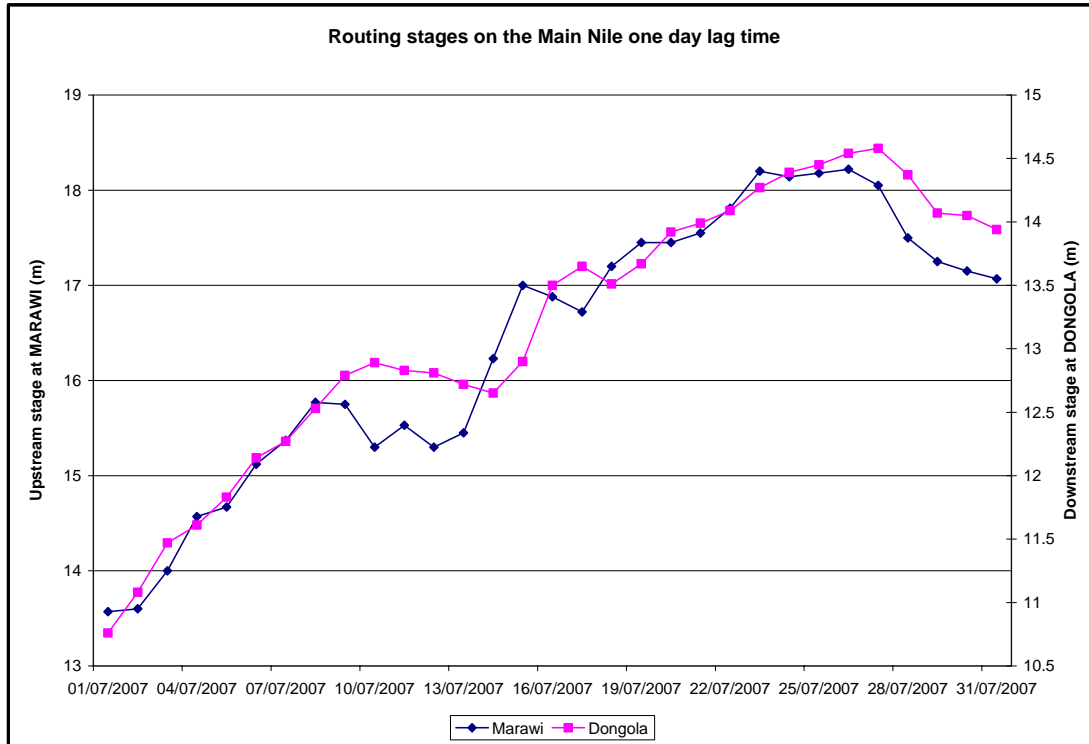
Figure 3.2a is time series hydrograph of Marawi station and Dongola stations and the data for July 2007. It can be seen one day lead time.

Figure 3.3b shows correlations between stage-stage on the River Blue Nile at Dongola

Figure (3.3b): coorelations between stage-stage on the Main Nile at Dongola
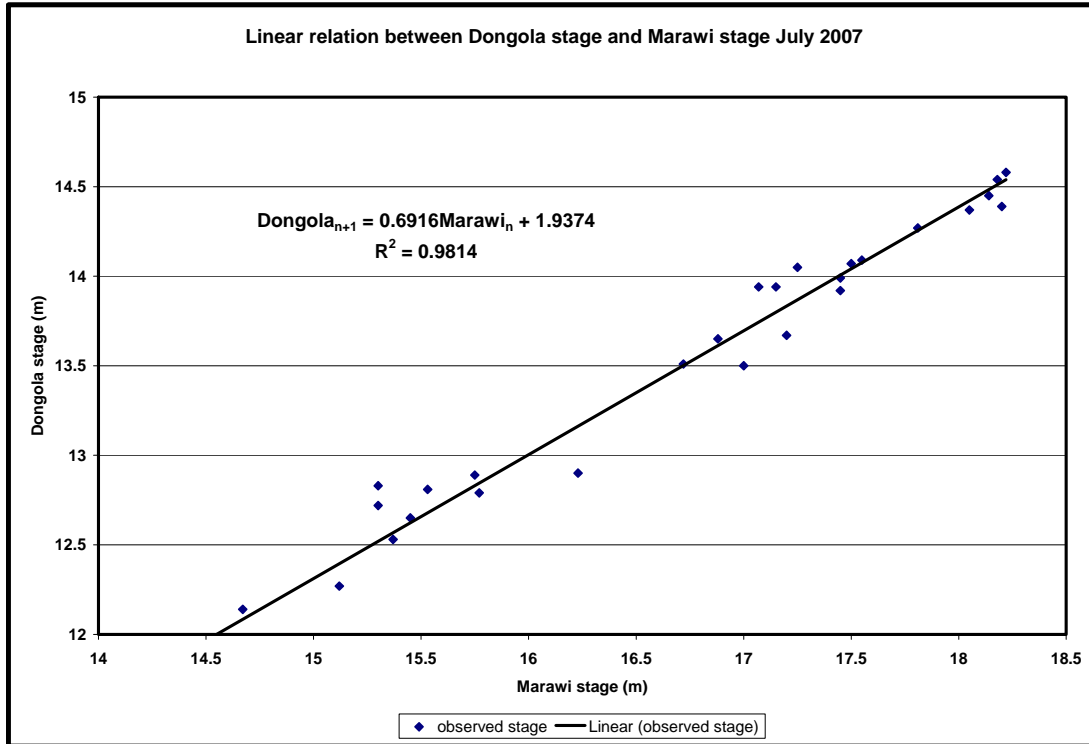
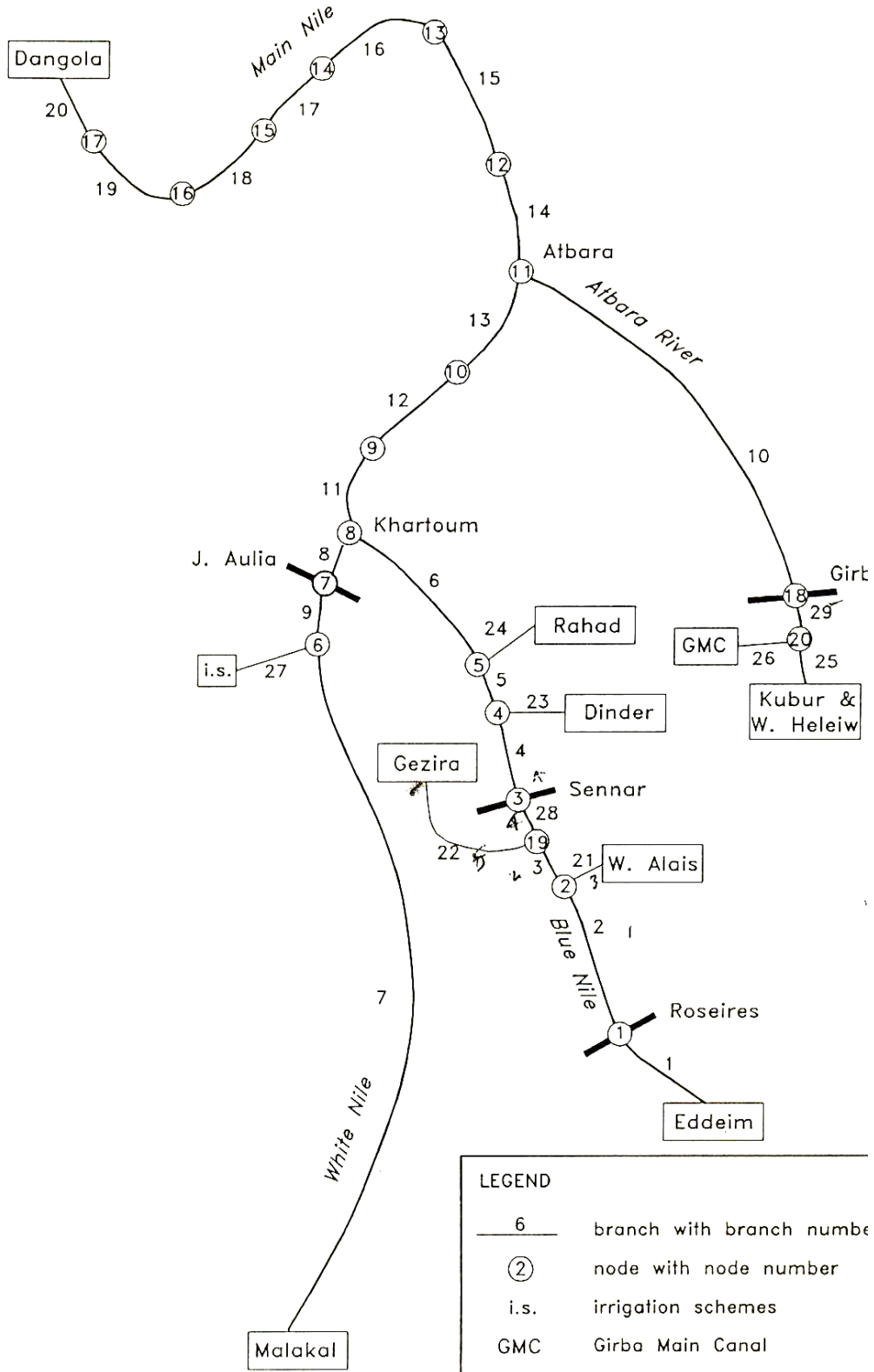It can be seen in figure 3.3b the correlation between the flows at Marawi and Dongla is excellent ($R^2 = 0.98$). This also it shows the good quality of data.

Figure: 3.4 boundary conditions for entering data

Chapter 4

Application, result and discussion

4.1 Introduction

The application and result of [FEWS] depends on the remote sensing and quality of cold cloud processing. The computation of the CCD for the processed images defined the number of hours the infrared brightness temperature is colder than a given temperature. The threshold temperature is varying for different types of rainfall situations.

Estimates of the areal daily average rainfall, derived from cloud cover duration (CCD) data are used in the flow routing to Eddeim. This has been done in order to facilitate the comparison of results of the simple routing and the SAMFILL model.

4.2 Discussion of Results

The statistical analysis was carried for more comparison between observed data and forecasted data, the range of data, the mean, the correlation and unpaired t test for comparing the actual difference between two means in relation to the variation in the data weather if similar group or not. Table 4.1 and figure 4.1 shows ten days areal Rainfall on Ethiopian plateau and Discharge at Eddeim

Table (4.1): Ten days areal Rainfall on Ethiopian plateau and Discharge at Eddeim

Period	Estimated Rainfall (mm) at B.nile Catchment	Real discharge (Mm^3)at Eddeim
Jul I	73	2981
II	49	4240
III	109	4211
Aug I	105	5633
II	88	5152
III	100	5762
Sep I	80	6289
II	95	5264
III	65	3873
Total	764	43405

Figure (4.1): Ten days areal Rainfall on Ethiopian plateau and Discharge at Eddeim
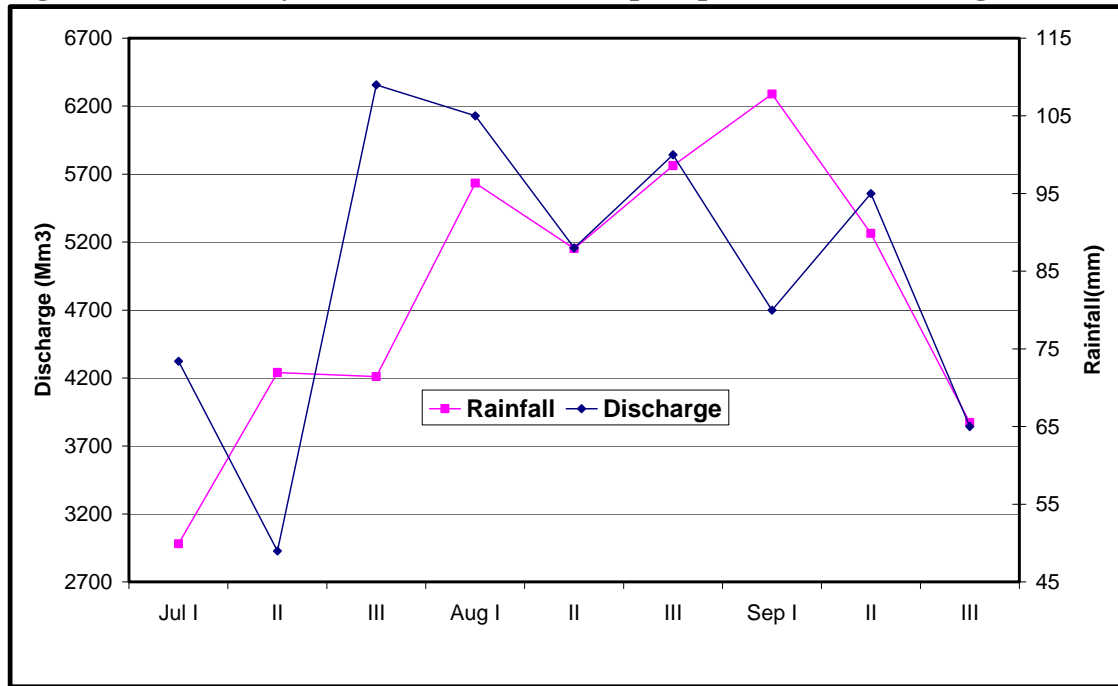
It is interesting to compare the sum of the ten-day flows of Eddeim station and sum ten-days of rainfall over Blue Nile catchments, there is some similarity.

It can be seen from the table 4.1 and figure 4.1 the ten –days total is nearly similar than daily simulation.

Figure (4.2): Rainfall-Runoff Modeling of Blue Nile at Eddeim
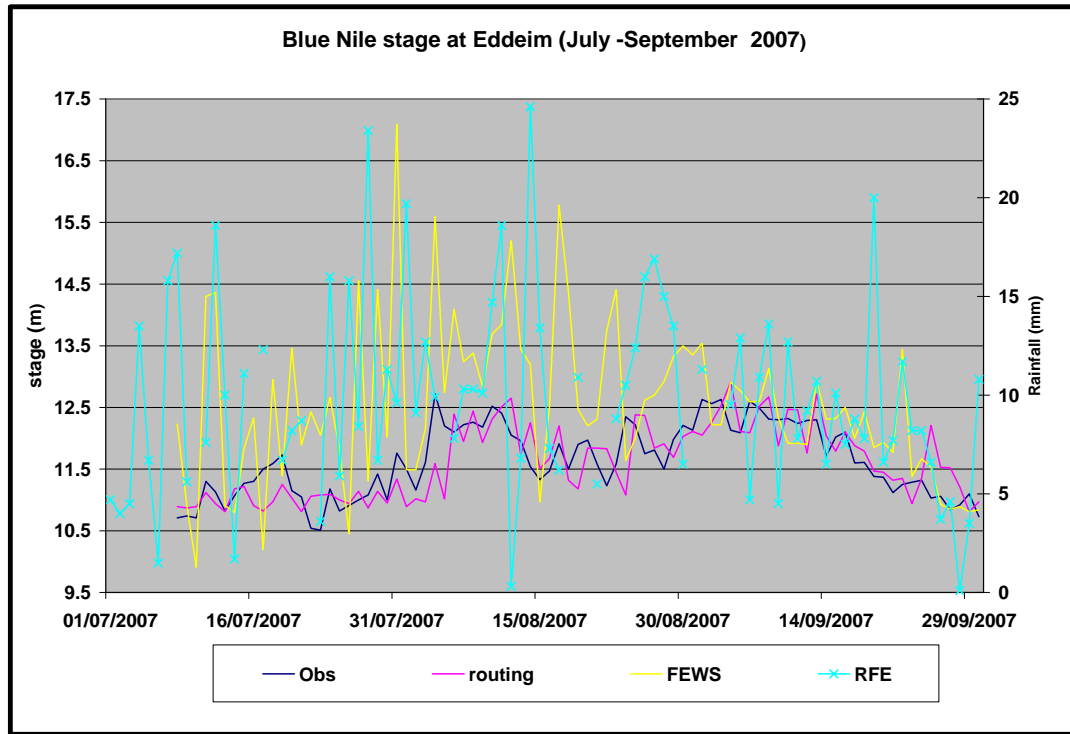
Figure 4.2 compare the observed stage at Eddeim with estimated stage using routing and FEWS model superimposed on them the rainfall estimated. It can be seen that simple routing reproduced the observed stages for better than the FEWS model.

Table (4.2): Summary of statistical values of model efficiencies for Blue Nile at Eddeim

Station	Eddeim		
	Output Data(m) from (July –September 2007)		
Parameter	Observed	Routing	FEWS
Max	12.72	12.91	17.09
Mean	11.63	11.60	12.54
Min	10.51	10.81	9.910
SD	0.5796	0.5883	1.2921
P value		0.784	0.0001
R^2		0.53	0.18

Table 4.2 shows sum summary statistic of the observed, routed and FEWS stages.

Figure (4.3): River Flow Modeling of Blue Nile at Khartoum

Figure 4.3 shows the coparison of the different stages for year 2007 in Khartoum.it can also be seen that the simple routing produced better result than FEWS.

Table 4.3 shows summary of statistical values of model efficiencies for B. Nile at Khartoum

Table (4.3): Summary of statistical values of model efficiencies for B. Nile at Khartoum

Station	Khartoum		
	Output Data(m) from (July –September 2007)		
Parameter	Observed	Routing	FEWS
Max	16.96	17.03	16.89
Mean	16.044	16.0295	15.7962
Min	13.4	13.4	13.66
SD	0.8195	0.8215	0.7482
P value		0.9086	0.0411
R^2		0.98	0.94

49

Figure (4.4): River flow modeling of Main Nile at Dongola

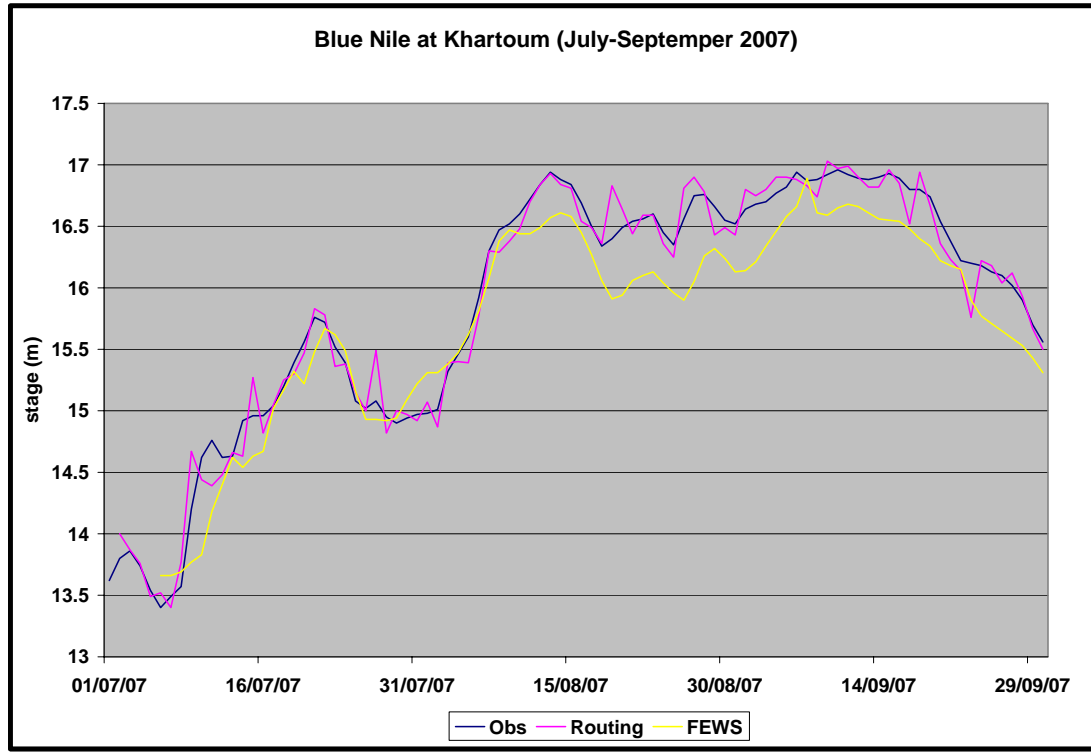Main Nile at Dongola (July - September 2007)
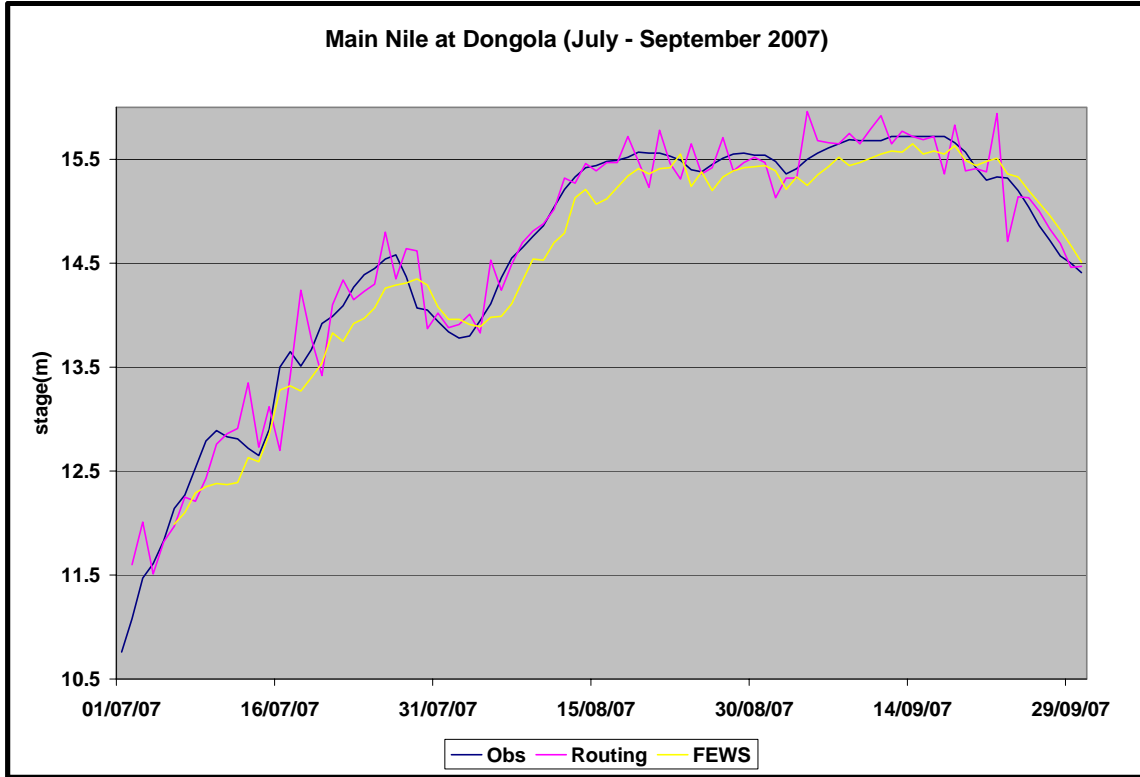
Figure 4.4 shows the comparison of the different stages for year 2007 in Dongola.it can also be seen that the simple routing produced better result than FEWS.

Table 4.4 shows summary of statistical values of model efficiencies for main Nile at Dongola.

Table (4.4): Summary of statistical values of model efficiencies for Main Nile at Dongola

Station	Dongola		
	Output Data(m) from (July –September 2007)		
Parameter	Observed	Routing	FEWS
Max	15.72	15.96	15.65
Mean	14.53	14.60	14.58
Min	10.76	11.51	11.99
SD	0.9286	0.9488	0.9704
P value		0.9188	0.3379
R^2		0.96	0.97

Table (4.1) comparison between estimated rainfall in (mm) on Ethiopian plateau and discharge at Eddiem shows one month lead time in reaching to summit, while the graph of rainfall have a gentle jump to reach its peak on first period sum of ten days on August which is 105mm, conversely the hydrograph of discharge rising gradually to approach its peak on the first period sum of ten days of the September which is 6289 million cubic meter, the two graphs simulated on second and third period of September.

Figure (4.2) the comparison of observed real data and those performances by FEWS models, Simple Routing and rainfall estimated by simple regression. The hydrograph reveals that performance of the simple routing is significantly better than that of the FEWS. Table (4.2) indicate the consistency in the performance of the FEWS model and simple routing through correlation coefficient examination, the fit of data simulated by FEWS is much worth (R^2 = 0.18) than simple routing (R^2 = 0.53) for Eddiem station. Also for comparing the means the student's t-test was carried so the actual difference between the mean of observed data and data computed by FEWS for Eddiem station the two-tailed P value is less than 0.0001 by conventional criteria, this difference is considered to be extremely statistically significant (real difference), for simple routing data the two-tailed P value equals 0.784 by conventional criteria, this difference is considered to be not statistically significant.

Figure (4.3) shows measured flow verse forecast results for the performance of the FEWS and simple non storage routing during the period 2007 flood season (1/7/2007 to 1/9/2007) for the Khartoum station. It can be seen from this figure that the FEWS model fits the observed stage hydrograph with a trivial under estimation but well simulation, compared to simple routing there is insignificant differences. It is notable that the estimated stage of simple routing has sharp fluctuations in over estimation. These fluctuations might be due to some storm between Madani and Khartoum stations.

Table (4.3) summaries the statistical values of models efficiencies for Blue Nile at Khartoum, the table shows the efficiencies of simple linear routing is (R^2 = 0.98), the FEWS is (R^2 = 0.94). However the FEWS performance is somewhat reverse to simple routing in the maximum record simple routing (+ 0.07 cm) and FWES (-0.07 cm) this may indicate some contributions to the river channel after point of entering boundary stations. Moreover the two-tailed P value equals 0.9086 for simple routing, which by

conventional criteria, this difference is considered to be statistically insignificant and the two-tailed P value equals 0.0411 for FEWS, which by conventional criteria, this difference is considered to be statistically significant.

Figure (4.4) shows river flow Modeling of main Nile at Dongola the performance of FEWS in simulation is better than simple routing (R^2 = 0.97) and (R^2 = 0.96) for FEWS and simple routing respectively, however the two-tailed P value equals 0.9188 for simple and the two-tailed P value equals 0.3379 for FEWS, and both the models by conventional criteria, this difference is considered to be not statistically significant.

Chapter Five

Summary, Conclusion and Recommendation

5.1 Summary

The data used in this study consist of areal daily rainfall over Ethiopian plateau (Five catchments) of period July -September 2007 for SAMFIL model and for the same period daily data of fourteen waterlevels measurements stations with four discharges from reservoirs and three offtakes is taken for NETFIL model and simple routing equations. The measured daily data is essential for a proper updating of the operation of the system. An update cycle consists of: prediction of rainfall from CCD-values, computation of the runoff from the catchments due to this rainfall, prediction of waterlevels, and flows in the entire river system and computation of coefficients. The model parameters were estimated from the model calibrated for the flood seasons of 1987-1990, as only for those years CCD-data were available to estimate catchments rainfall. For simple non-storage routing the parameters is updated day by day according to change in time and x-section.

5.2 Conclusion

It can be concluded that simple Non-storage Routing method, whichever is very approximate method, but gives better performance than FEWS for the three selected station. For real-time river flow forecasting at ELdeim station on the Blue Nile River. The comparison of performance is carried out for the flood season of 2007; Rainfall estimates derived from the Cold Cloud Duration (CCD) are used in the comparison. The results in general show that the discharge forecasts of the Simple non-storage Routing method is more reliable than those of the FEWS on the basis of the simulation and consistency ($R^2 = 0.18$) compared to simple routing ($R^2 = 0.53$). The actual difference between the mean observed and computed carried by t-test indicated extremely statistically significant difference for those computed by FEWS. From the visual comparison of the observed and estimated discharge hydrographs it is clear that FEWS has an exaggerating oscillatory shape it is reflects some numerical instability problems in the updating procedure likely that the interior performance of inadequacy of the extended

Kalman Filter updating procedure. On the other hand, the simple linear regression parameter and type of Cold Cloud Duration (CCD) is not perfect.

Generally the performance of the FEWS is not bad and the performance of Simple Non-storage Routing is good for both stations at Khartoum and Dongla. The consistency and simulation for Khartoum station is ($R^2 = 0.98$) & ($R^2 = 0.94$) for Simple Routing Method and FEWS respectively which indicate good simulation. On the other side the difference of mean P value is (0.9086) & (0.411) which indicate the insignificant difference for simple routing. Also visual hydrograph inspection reveals the under estimation resulted from FEWS. For Dongola station the performance of FEWS is little better in simulation than simple routing method, although still poor performance of FEWS in mean difference.

5.3 Recommendation

- The Simple Non-Storage Routing can be used as forecasting method when the hydrograph of two stations is plotted and it depend on time and quantity of flood peak, on other word flood translation and attenuation between upstream and downstream stations should be well defined.

- For climatologically boundary conditions, point stations for both rainfall and evapotranspiratin are strongly needed with well distribution on all the catchments to represent every segment in order to calibrate areal rainfall.

- For hydrological boundary conditions, rating equations and reservoir content, needs a regular update.

- For rainfall-runoff modeling, the spatial distribution of rainfall requires additional segmentation of Blue Nile. Also information like topography, soil, vegetation as well as point rainfall, avaporation, water level and discharge data for Ethiopian and Eritrean parts of the Blue Nile, Atbara and Setit are well needed for purpose to improve Extended Kalman filter performance.

References

1. Shaw, E. M. (1994). *Hydrology in Practice*: Flood Routing. Chapman &Hall, 3rd Ed, UK, 401 pp.

2. Barsi,B.I.(1986). Interna. Confer. On water Resources Needs & Planning in Drouht Prone Areas- Khartoum Dec.1986: A Flood Routing Method for Seasonal Rivers, 12-13 pp.

3. Shamseldin, A.Y.; Abdo, G.M. and Elzein, A.S (1997). Sudan Engineering Society JOURNAL, July 1998 Vol. 45, No.36: Real Time Flood Forecasting on the Blue Nile, 20-22 pp.

4. Sutcliffe, J.V.; Dugdale, G. and Milford, J.R (1989). Hydrological Sciences – des Sciences Hydrologiques, 34, 3, 6/1989,UK: Technical note on the Sudan Flood 1988, 355-359 pp.

5. Manusthiparom, Dr.C. & Apirumanekul, Dr.C (2005). Flood Forecasting and River Monitoring System in the Mekonge River Basin: Second Southeast Asia Water Forum, August 29th –September 3rd, Bali, Indonesia, 1-3 pp

6. WMO.(1986). Interna. Confer. on water Resources Needs & Planning in Drouht Prone Areas- Khartoum Dec.1986: Hydrological Modelling and Real-Time Forecasting in the Nile Basin, 81 pp

Ministry of Irrigation & Water Resources (MOIR), reports & technical Documents

7. Sudan Flood Early Warning System, FEWS final report December   1992.

8. Sudan Flood Early Warning System, FEWS final report February 1994.

9. WENDY version 3.00, V, 1&2 January 1991.

10. User Manual Flood Early Warning System Sudan.

11. Sub-Saharan Africa, Hydrological Assessment (Group 1 Countries),

    Final Report, Sudan, Octoober 1989.

Appendix 1

Model Parameters

PXADJ   Precipitation adjustment factor

PEADJ   ET-demand adjustment factor

UZTWM   Upper zone tension water capacity (mm)

UZFWM   Upper zone free water capacity (mm)

UZK   Fractional daily upper zone free water withdrawal rate

PCTIM   Minimum impervious area (decimal fraction)

ADIMP   Additional impervious area (decimal fraction)

RIVA   Riparian vegetation area (decimal fraction)

ZPERC   Maximum percolation rate coefficient

REXP   Percolation equation exponent

LZTWM   Lower zone tension water capacity (mm)

LZFSM   Lower zone supplemental free water capacity (mm)

LZFPM   Lower zone primary free water capacity (mm)

LZSK   Fractional daily supplemental withdrawal rate

LZPK   Fractional daily primary withdrawal rate

PFREE   Fraction of percolated water going directly to

                     lower zone free water storage

RSERV   Fraction of lower zone free water not transferable to

                     lower zone tension   water

SIDE   Ratio of deep recharge to channel baseflow

ET Demand   Daily ET demand (mm/day)

PE Adjust   PE adjustment factor for 16th of each month

ADIMC   Tension water contents of the ADIMP area (mm)

UZTWC   Upper zone tension water contents (mm)

UZFWC   Upper zone free water contents (mm)

LZTWC   Lower zone tension water contents (mm)

LZFSC   Lower zone free supplemental contents (mm)

LZFPC   Lower zone free primary contents (mm)